A NEW EXTENSION TO

THE SHADOW FILTER THEORY

BY

NAIF RADHYAN AL-MUTAIRI

A Thesis Presented to the

DEANSHIP OF GRADUATE STUDIES

KING FAHD UNIVERSITY OF PETROLEUM & MINERALS

DHAHRAN, SAUDI ARABIA

In Partial Fulfillment of the

Requirements for the Degree of

MASTER OF SCIENCE

In

ELECTRICAL ENGINEERING

May 2015

KING FAHD UNIVERSITY OF PETROLEUM & MINERALS

DHAHRAN- 31261, SAUDI ARABIA

DEANSHIP OF GRADUATE STUDIES

This thesis, written by **Naif Radhyan Al-Mutairi** under the direction his thesis advisor and approved by his thesis committee, has been presented and accepted by the Dean of Graduate Studies, in partial fulfillment of the requirements for the degree of **MASTER OF SCIENCE IN ELECTRICAL ENGINEERING.**

Dr. Abu El-Ma'atti, M. T.
(Advisor)

Dr Al-Shaikhi, Ali Ahmad
Department Chairman

Dr. Al-Absi, Munir A. K.
(Member)

Dr. Salam A. Zummo
Dean of Graduate Studies

Dr. Hussein, Alaa El-Din
(Member)

26/5/15

Date

I dedicate this work to my parents who always supporting me by continuous encouragement and most importantly their supplications to Allah to succeed in my life and the hereafter.

Also, I dedicate this work to my wife whom I can't forget her support to me

ACKNOWLEDGMENTS

Foremost, I am very grateful to Allah Almighty alone who is helping me to complete my master's thesis.

I am also grateful to my parents who always supporting me by their supplications to Allah day and night to succeed in my life and the hereafter. My sincere thanks go to my wife that gave me moral support at the bad moments during my research.

In addition, I would like to express my sincere gratitude to my advisor Prof. Muhammad Abu-El-Ma'atti for his continuous support during my studying in the MS. Degree and my research, also for his patience, his motivation and his guidance which helped me a lot in the research and writing of this thesis.

Finally, I place on record, my thanks to my friends: Zainulabideen, Eyas, Mohanad and Rakan for their support and attention as well as their enriching discussion in my research problems.

TABLE OF CONTENTS

LIST OF TABLES

LIST OF FIGURES

LIST OF ABBREVIATIONS

DISO: Double input single output

MISO: Multi-input single output

SIMO: single input Multi-outputs

ABSTRACT

Full Name : [Naif Radhyan Al-Mutairi]

Thesis Title : [An Extension to The Shadow Filters Theory]

Major Field : [Electrical Engineering]

Date of Degree : [April 2015]

The shadow filter theory was proposed in 2010. It was about changing the center frequency of a band pass filter by acting on an external amplifier. The shadow filtering provide great features where some of the filter parameters can be tuned externally without touching the passive or active components of the filter itself. The requirements of the shadow filter, proposed in 2010, are a 2^{nd} order filter, feedback amplifier as well as a summing circuit at the input. This work is an extension to the theory where the shadow filtering is achieved only by 2^{nd} order filter and a feedback amplifier without need to the an externally connected summing circuit. In addition to that, the shadow filter theory is extended to other types of filters. For example, the concept of the shadow filtering theory is utilized to tune the bandwidth and the center frequency independently for the band-pass filters and band stop filters. Moreover, the same concept is applied on the low pass and high pass filters to tune the center frequency with and without control over the quality factor.

ملخص الرسالة

الاسم الكامل: نايف رضيان تريحيب المطيري

عنوان الرسالة: إمتداد لنظرية مرشحات الظل

التخصص: الهندسة الكهربائية

تاريخ الدرجة العلمية: رجب 1436

في عام 2010 ظهرت نظرية مرشحات الظل. هذه النظرية تتكلم عن مرشحات تمرير النطاق وكيفية تغيير ترددها المركزي عن طريق التحكم بمقدار الكسب الكهربائي للمضخم الذي يصل بين الخارج والداخل بدائرة الجمع. هذا البحث هو إمتداد لنظرية مرشحات الظل, حيث تم تعميم النظرية على أنواع أخرى من المرشحات كمرشح تمرير الترددات المنخفظه ومرشح تمرير الترددات العالية ومرشح حجب النطاق. كما أنه في هذا البحث تم إقتراح تصميم لمرشحات الظل أقل كلفة من التصميم المقترح في 2010 حيث أنه لا حاجة لدائرة الجمع في التصميم المقترح.

CHAPTER 1

INTRODUCTION

In 2010, Y. Lakys and A. Fabre proposed for the first time the theory of the shadow filter [1]. It is a new family of second order analog filters. The concept of the shadow filter is based on changing the characteristic frequency of the 2^{nd} order filter by acting on the gain of an external amplifier.

In the shadow filter, acting on the external amplifier's gain lead to a change in the center frequency of the band-pass filter while the quality factor will adapt its value to maintain constant bandwidth. This feature is achieved without modifying the passive and active components of the filter. This approach is very useful in designing the reconfigurable filters where the center frequency is varying over a wide frequency range. Moreover, the hop between two consecutive bands will be carried out very quickly during the signal transmission. In addition to that, electronic fine tuning of the filter parameters using this approach can be very attractive to compensate for the non-ideal effects.

If the external amplifier's gain is controlled by a DC current or voltage, the analog signal will be saved from the distortion resulting from switches because the switching is in the dc domain. Contrary to other tuning techniques, such as the switched capacitors technique where the tuning is done via the switching frequency and in this case the analog signal will suffer from the switching distortion.

The idea of the shadow filter can be extended to two interesting characteristics depending on which output port is feeding the feedback amplifier. The two interesting characteristics are tuning the bandwidth with tuning or fixing the center frequency. Also, tuning the center frequency and bandwidth with fixing the quality factor.

CHAPTER 2

LITERATURE REVIEW

2.1 Shadow Filters

In 2010, Y. Lakys and A. Fabre proposed a shadow filter [1]. It is a new family of second order analog filters. The idea of the shadow filter is based on changing the characteristic frequency of the 2nd order filter by acting on the gain of an external amplifier.

Consider the second order filter in Fig.1 with the transfer functions:

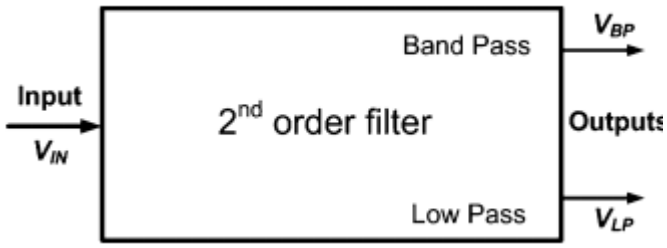

Fig. 1: Basic 2nd order filter [1]

$$\mathbf{F_{BP}(s)} = \frac{\mathbf{V_{BP}}}{\mathbf{V_{IN}}} = \frac{\boldsymbol{a's}}{\mathbf{1} + \boldsymbol{as} + \boldsymbol{bs^2}} \quad (1)$$

$$\mathbf{F_{LP}(s)} = \frac{\mathbf{V_{LP}}}{\mathbf{V_{IN}}} = \frac{\boldsymbol{d'}}{\mathbf{1} + \boldsymbol{as} + \boldsymbol{bs^2}} \quad (2)$$

Note that all the constant (a, b, a' and d') are real and positive.

If the low pass output is amplified by external amplifier of gain **A** and then added to the V_{IN} so that the $V_E = V_{IN} - AV_{LP}$ as shown in Fig.2:

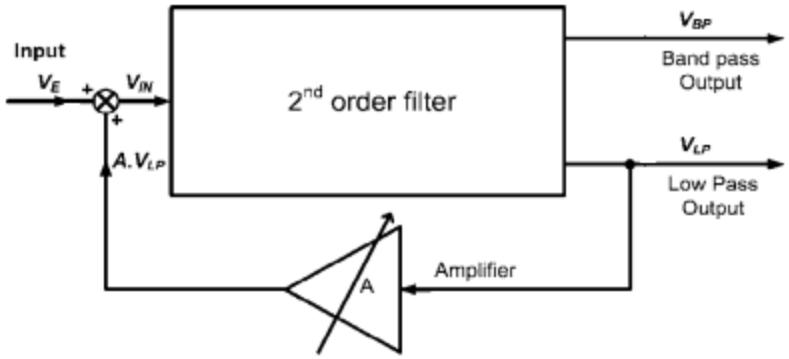

Fig. 2: 2nd order shadow filter [1]

The transfer function of the bandpass filter is now given by Eq(3):

$$\mathbf{F_{BPA}(s)} = \frac{\mathbf{V_{BP}}}{\mathbf{V_E}} = \frac{\frac{a's}{1-Ad'}}{1 + \frac{as}{1-Ad'} + \frac{bs^2}{1-Ad'}} \quad (3)$$

Table.1 shows the different between the basic 2nd order filter and the shadow filter in terms of the filters' parameters:

Table 1: Filter Characteristics of Fig.1 and Fig.2

	Basic 2nd order filter (Fig.1)	***Shadow filter (Fig.2)***
Center frequency	$\boldsymbol{f_o = \frac{1}{2\pi\sqrt{b}}}$	$\boldsymbol{f_{oA} = f_o\sqrt{1-Ad'}}$
Q-factor	$\boldsymbol{Q = \frac{\sqrt{b}}{a}}$	$\boldsymbol{Q_A = Q\sqrt{1-Ad'}}$
Bandwidth	$\boldsymbol{BW = \frac{a}{2\pi b}}$	$\boldsymbol{BW_A = BW = \frac{a}{2\pi b}}$
BP Gain	$\boldsymbol{G_{BP} = \frac{a'}{a}}$	$\boldsymbol{G_{BPA} = GBP}$
LP Gain	$\boldsymbol{G_{LP} = d'}$	$\boldsymbol{G_{LPA} = \frac{G_{LP}}{\sqrt{1-Ad'}}}$

It is clear from Table.1 that the characteristic frequency can be tuned by the gain of the external amplifier provided that ($1 - Ad'$) is positive. Fig.3 shows the center frequency of the shadow filter versus the gain of the amplifier **A**.

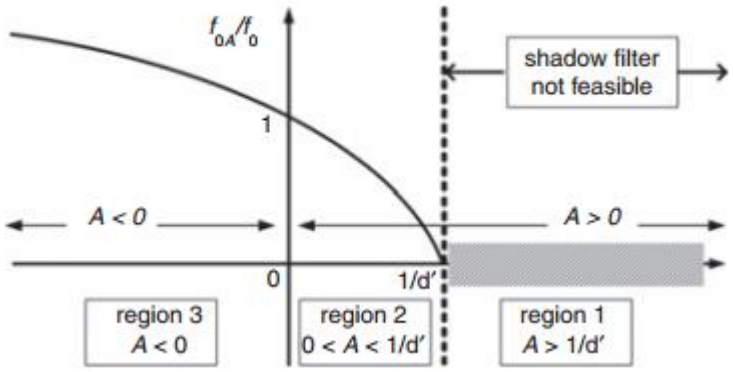

Fig. 3: foA/fo variation Vs Gain of amplifier [1]

When the gain of the amplifier is negative, the center frequency of the shadow filter (fo_A) will be greater than the center frequency of the starting filter (*fo*); that's in region 3. However, if the gain of the amplifier is positive and less than 1/d', fo_A will be smaller than *fo* as shown in region 2. While the shadow filter is not feasible in region 1.

2.2 Nth Order Shadow Filters:

The idea of the shadow filters has been generalized to class-n shadow filters [2] by the same authors, where the center frequency of the nth order shadow filter will be

$$f_{oA} = f_o(1 - Ad')^{\frac{n}{2}}$$

Fig.4 shows the class-1 shadow filter, where the basic 2nd order filter (starting filter) is now called class-0 shadow filter.

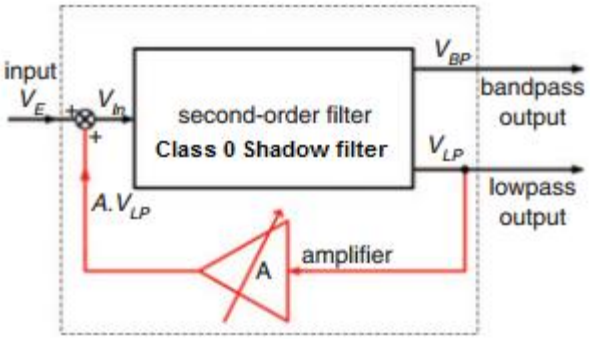

Fig. 4: Class 1 Shadow Filter [2]

N[th] order shadow filter can be realized if the low pass signal is amplified by N number of amplifiers and summing them with the input signal. For each amplifier in the feedback, there must be an amplifier with gain (1-Ad') in the low pass output to compensate for the low pass gain (G_{LP}) reduction as it is illustrated in Fig.5

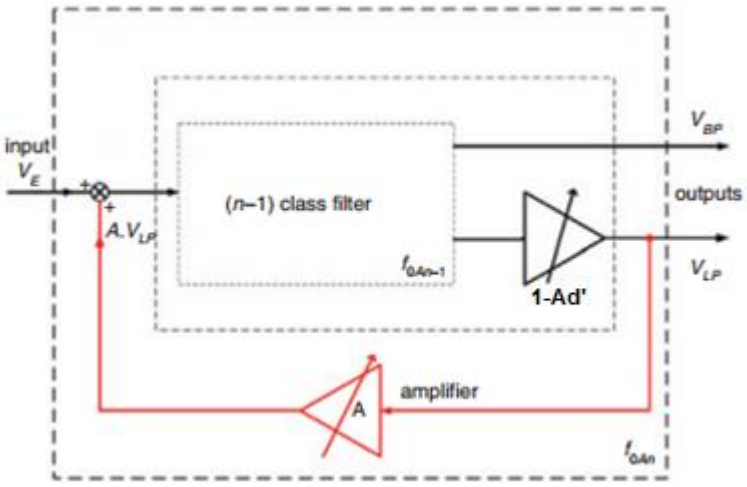

Fig. 5: Nth Order Shadow Filter [2]

Table.2 shows the n[th] order shadow filter parameters compared with the starting filter.

Table 2: Filter Charactrisctics of Fig.5 and Fig.1

	Basic 2nd order filter (Fig.1)	*Nth Order Shadow filter (Fig.5)*
Center frequency	$f_O = \frac{1}{2\pi\sqrt{b}}$	$f_{OAn} = f_O(1 - Ad')^{\frac{n}{2}}$
Q-factor	$Q = \frac{\sqrt{b}}{a}$	$Q_{An} = Q(1 - Ad')^{\frac{n}{2}}$
Bandwidth	$BW = \frac{a}{2\pi b}$	$BW_{An} = BW$
BP Gain	$G_{BP} = \frac{a'}{a}$	$G_{BPAn} = G_{BP}$
LP Gain	$G_{LP} = d'$	$G_{LPAn} = \frac{G_{LP}}{\sqrt{1 - Ad'}}$

Fig.6 shows the variation of f_{OAn} / f_n versus the gain of the external amplifiers for different values of n (the order of the shadow filter). When A is negative (region 3) f_{0An} is greater than f_0 and its increasing is even faster as n is greater. While for n=2, the evolution is a linear function. However, the filter is not feasible for A greater than 1.

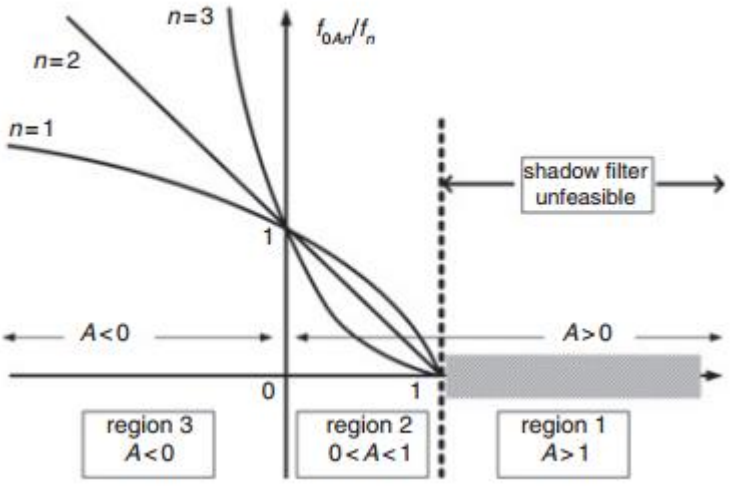

Fig. 6: f_{oAn} / f_n versus A ; for several values of n [2]

2.3 requency Agile Filters (FAF):

In the literature, the frequency agile filter is a reconfigurable filter where the hop between two bands (from f_1 to f_2) is carried out very quickly during the transmission of the signal [3].

Assuming the center frequency is adjustable between two values: $f_{O\text{Min}}$ and $f_{O\text{Max}}$, the adjustment range is defined in [3] as the ratio between $f_{O\text{Max}}$ *and* $f_{O\text{Min}}$:

$$n = \frac{f_{O\text{Max}}}{f_{O\text{Min}}}$$

The tunable filter in [3] is the filter whose tuning of *fo* is around *fo* to compensate for the drift in the center frequency *fo* due the non-ideality and other factors or in other words: $f_{O\text{Max}} < 2f_{O\text{Min}}$.

While the reconfigurable filter is the filter whose center frequency is expected to be tuned over a wide range of frequencies; or in other words: $f_{O\text{Max}} > 2f_{O\text{Min}}$.

2.4 Circuit Implementation:

In [4], The authors proposed a current mode shadow filter based on ZC-CITA (Z-Copy Current Inverter Transconductance Amplifier). The outputs of the high pass filter and bandpass filter are also amplified and summed to the input, where the gain of the amplifiers in the low pass feedback and the bandpass feedback are used to tune the bandwidth and the center frequency independently. They used two ZC-CITAs and two

current amplifiers. However, a current buffer or a current mirror is needed to take the band-pass output current.

In [5] and [10] CDTA(current differencing trans-conductance amplifier) frequency agile filter (FAF) was proposed. The authors in [5] proposed three circuits to realize class-0, class-1 and class-2 FAF based on CDTA. They used two CDTAs, two CDTAs and one trans-conductance amplifier and two CDTAs and three trans-conductance amplifiers respectively. While in [10] only two classes of FAF are introduced; one is class-0 FAF (simple band-pass filter) consisting of one CDTA, two grounded capacitors and one floating resistor. While class-1 FAF consists of and two CDTA, two grounded capacitors and two resistors. However, in [5] and [10] the band-pass output current can't be taken without current buffer or current mirror. Authors in [10] extended the idea of class-0, class-1 and class-2 FAF to VDTA (voltage differencing trans-conductance amplifier) and their proposed circuits consist of one VDTA , two VDTAs and three VDTAs respectively. The simulation results for [5] and [10] are based on simulations using 0.25μm TSMC CMOS technology model parameters. The performance of the FAF of [5] and [10] are evaluated in terms of power dissipation, SNR and output noise voltage.

Fabre and Lakys in [3],[6] and [8] proposed class-1 FAF based on CCCII+. The class-0 FAF contains 3 CCCII+ as well as 2 capacitors. The low pass output is fed into three parallel CCCII+ configured as current amplifiers. The gain of the current amplifier is controlled by its biasing current which is controlled by switch. The adjustment ratio was $n = 5.1$ where $f_{O\mathrm{Min}} = 239.7\ MHz\ and\ f_{O\mathrm{Max}} = 1.223GHz$. The same authors in [7] proposed the same class-0 FAF. However, there is a set of four current amplifiers

where their biasing current is digitally controlled. Based on the digital input, class-1 FAF, class-2 FAF and class-3 FAF can be achieved.

Dutta Roy in [7] extended the idea of the shadow filters. He suggested taking the feedback from the high pass output to get higher Q quality factor at lower frequencies as well as taking the feedback from the band-pass filter to get variable Q with constant center frequency. Moreover, the author raised a question about the possibility of having constant Q with a variable center frequency.

CHAPTER 3

PROPOSED WORK

Fabre and Lakys proposed the shadow filter [1] based on the single-input dual-output filter. Thus the block diagram of Fabre's scheme shown in Fig.7 consists of:

- 2^{nd} order filter
- Amplifier in the feedback path
- Summing circuit to sum the input signal with feedback signal

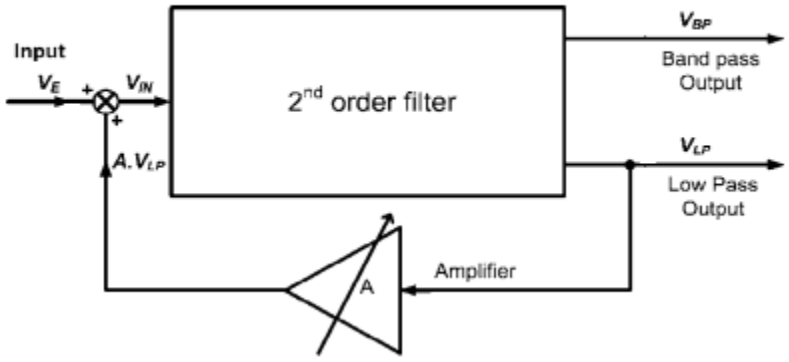

Fig. 7: Class-1 shadow filter [1]

Now, let us consider dual-input single-output 2^{nd} order filter as shown in Fig.8 Assuming A, B, a and b are real positive, the transfer functions given by eq.4:

Fig. 8: Dual Inputs Single Output Filter

$$V_O = \frac{AsV_1 + BV_2}{as^2 + bs + 1} \quad (4)$$

Table 3: Filter characteristic of Fig.8

Center Frequency	*Bandwidth*	*Band pass Gain (V2=0)*	*Low Pass Gain (V1=0)*
$f_O = \frac{1}{2\pi}\sqrt{\frac{1}{a}}$	$BW = \frac{b}{2\pi a}$	$G_{BPF} = \frac{Aa}{b}$	$G_{LPF} = Ba$

3.1 New Extension to the Shadow Filters Theory

A new proposed scheme for the shadow filter is shown in Fig.9 which can be considered a new extension to the shadow filters theory.

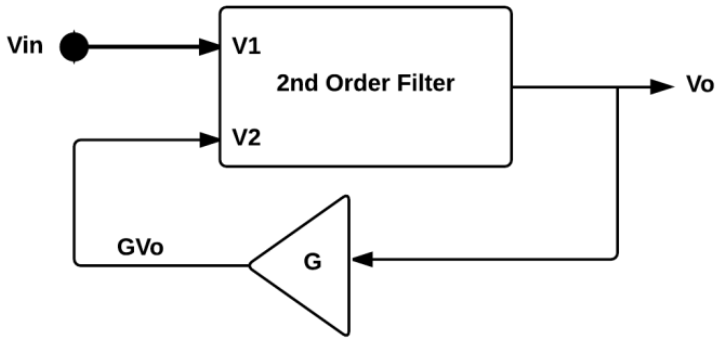

Fig. 9: New type of class-1 shadow filter

Theoretical approach: Assuming A, B, a and b are real positive:

$$V_O = \frac{AsV_{in} + GBV_O}{as^2 + bs + 1} \quad (5)$$

$$\rightarrow \quad V_O\left[1 - \frac{GB}{as^2 + bs + 1}\right] = \frac{AsV_{in}}{as^2 + bs + 1} \quad (6)$$

$$\rightarrow \quad V_O = \frac{AsV_{in}}{as^2 + bs + 1 - GB} \quad (7)$$

➔ $$V_O = \frac{\frac{AsV_{in}}{1-GB}}{\frac{a}{1-GB}s^2 + \frac{b}{1-GB}s + 1} \quad (8)$$

Table 4: Filter characteristics of Fig.9

Center Frequency	*Bandwidth*	*Band pass Gain*
$f_O = \frac{1}{2\pi}\sqrt{\frac{1}{a}}\sqrt{1-GB}$	$BW = \frac{b}{2\pi a}$	$G_{BPF} = \frac{Aa}{b}$

Table.5 shows the comparison between the Fabre's scheme and the proposed scheme:

Table 5: Comparison between Fabre's scheme and the proposed scheme

	Fabre's Scheme	Proposed Scheme
2nd Order Filter	Yes	Yes
Feedback Amplifier	Yes	Yes
Summing Circuit	Yes	No

The main advantage of the proposed shadow filter over Fabre's scheme is that no need for summing circuit at the input signal where the amplified feedback signal will be fed to another input (V_2: the input which will produce the low pass charactristic at the output).

Fabre's shadow filter scheme consists of two output ports; low pass port and bandpass port, so, in the current mode filters, using the Fabre's scheme is preferable because sampling and mixing the current will be easier. While in the proposed scheme, a current mirror is needed to sample the output current.

However, in the voltage mode filters, the proposed design is preferred compared to the fabre's scheme because no need for using summing circuit with the input voltage.

3.1.1 Practical Verification for the proposed scheme of the shadow filters:

To verify the new scheme of the shadow filter, a dual input single output CFOA based filter, which is a modified version of the circuit proposed in [9], is implemented as shown in Fig.10

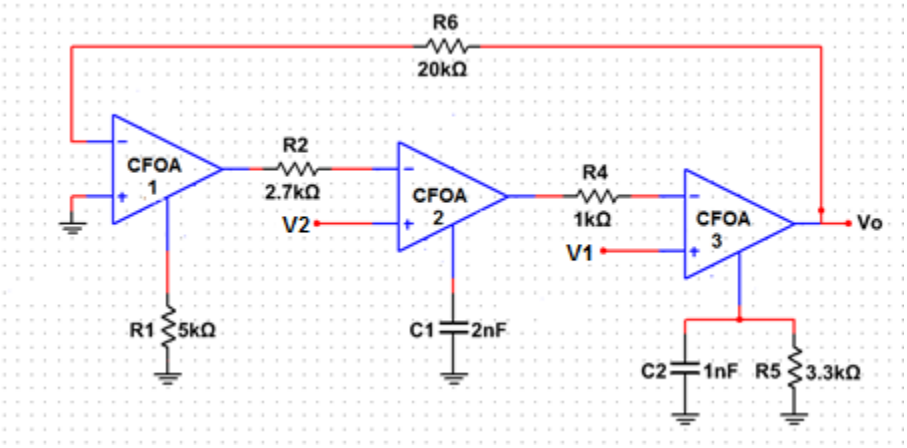

Fig. 10: Dual input single output CFOA filter [9]

The transfer function is:

$$V_O = \frac{-\frac{1}{R_2 R_4 C_1 C_2} V_2 + s\frac{1}{R_4 C_2} V_1}{s^2 + s\frac{1}{C_2 R_5} + \frac{R_1}{R_2 R_4 R_6 C_1 C_2}} \quad (9)$$

This filter is implemented in NI ELVIS II+ breadboad, the NI ELVIS hardware are accessed through measurement instruments that are accessed, viewed and controlled from the PC.

The experimental results are shown in Fig.11 and summarized in Table 6:

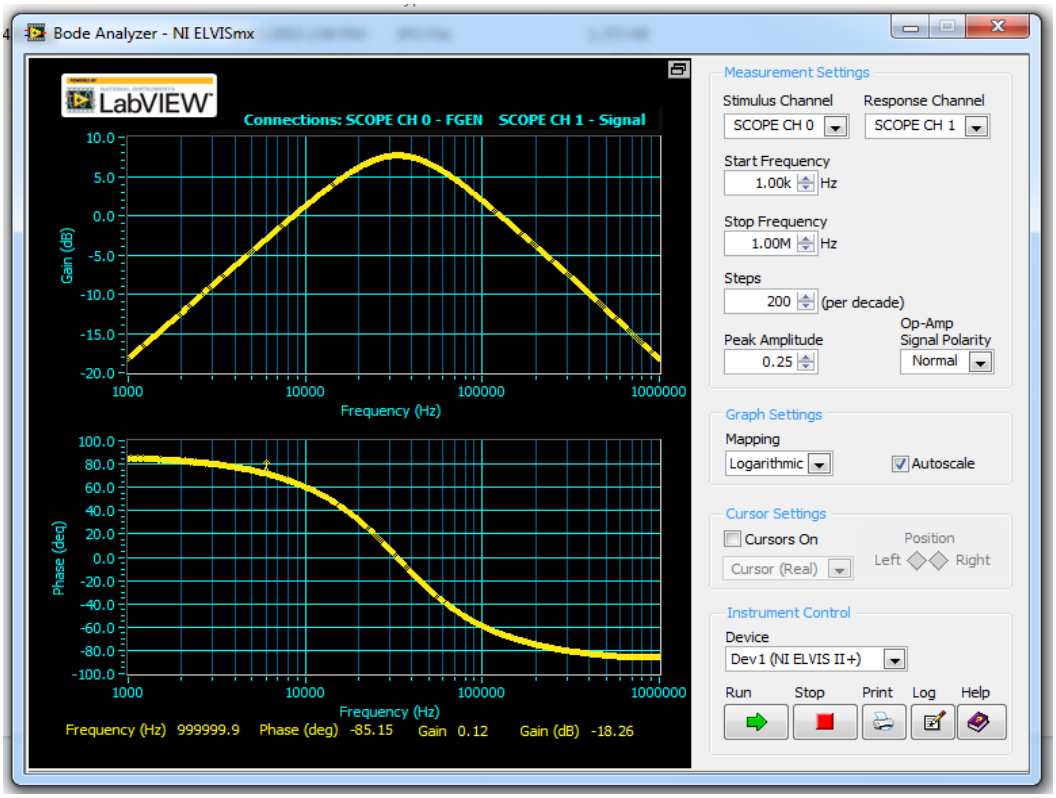

Fig. 11: Gain and phase frequency response

Table 6: The theoretical and experimental results of Fig.10

	Center Frequency	***Bandwidth***	***Band pass Gain***
Theoretically	***34.2KHz***	***48 KHz***	**3.3**
Experimentally	***34.7 KHz***	***56 KHz***	**2.6**

After taking the measurement of the filter charactristcs, the shadow filtering is applied by amplifying and feeding the output volatage to V_2 (the input voltage that produce low pass output) as shown in Fig.12.:

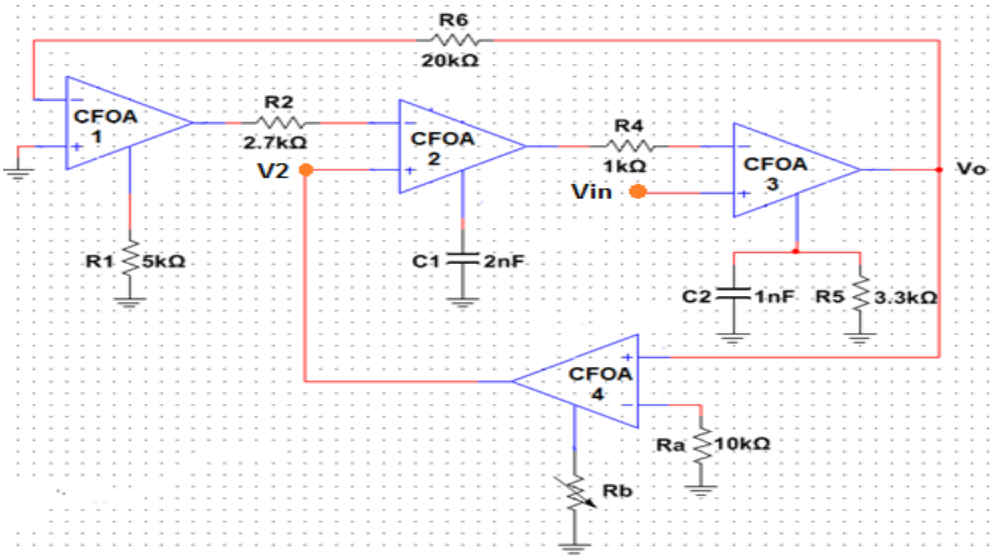

Fig. 12: Class-1 shadow filter

$$V_O = \frac{s\frac{1}{R_4C_2}V_{in}}{s^2 + s\frac{1}{C_2R_5} + \frac{R_1}{R_2R_4R_6C_1C_2}\left(1 - A\left(-\frac{R_6}{R_1}\right)\right)} \qquad (10)$$

Circuit in Fig.12 is implemented in NI ELVIS II+ breadboard. Then, the circuit is tested under several values of the feedback voltage amplifier gain (0, 1,2,3 and 4), where $(-\boldsymbol{R_6/R_1})$ represents the gain of low pass filter when V_1 is set to zero. While $\boldsymbol{A = R_b/R_a}$ repesents the gain of the amplifier. Table 7 shows the experiemental results.

Table 7: The experiemental results of class-1 shadow filter in Fig.12

Amplifier Gain (A)	$(-\boldsymbol{R_6/R_1})$	Center frequency	BW	Gain of BPF
0	-4	34.7 KHz	56 KHz	2.6
1	-4	81 KHz	62 KHz	2.4
2	-4	100 KHz	62 KHZ	2.4
3	-4	130 KHz	52 KHz	2.8
4	-4	146 KHz	53 KHz	3

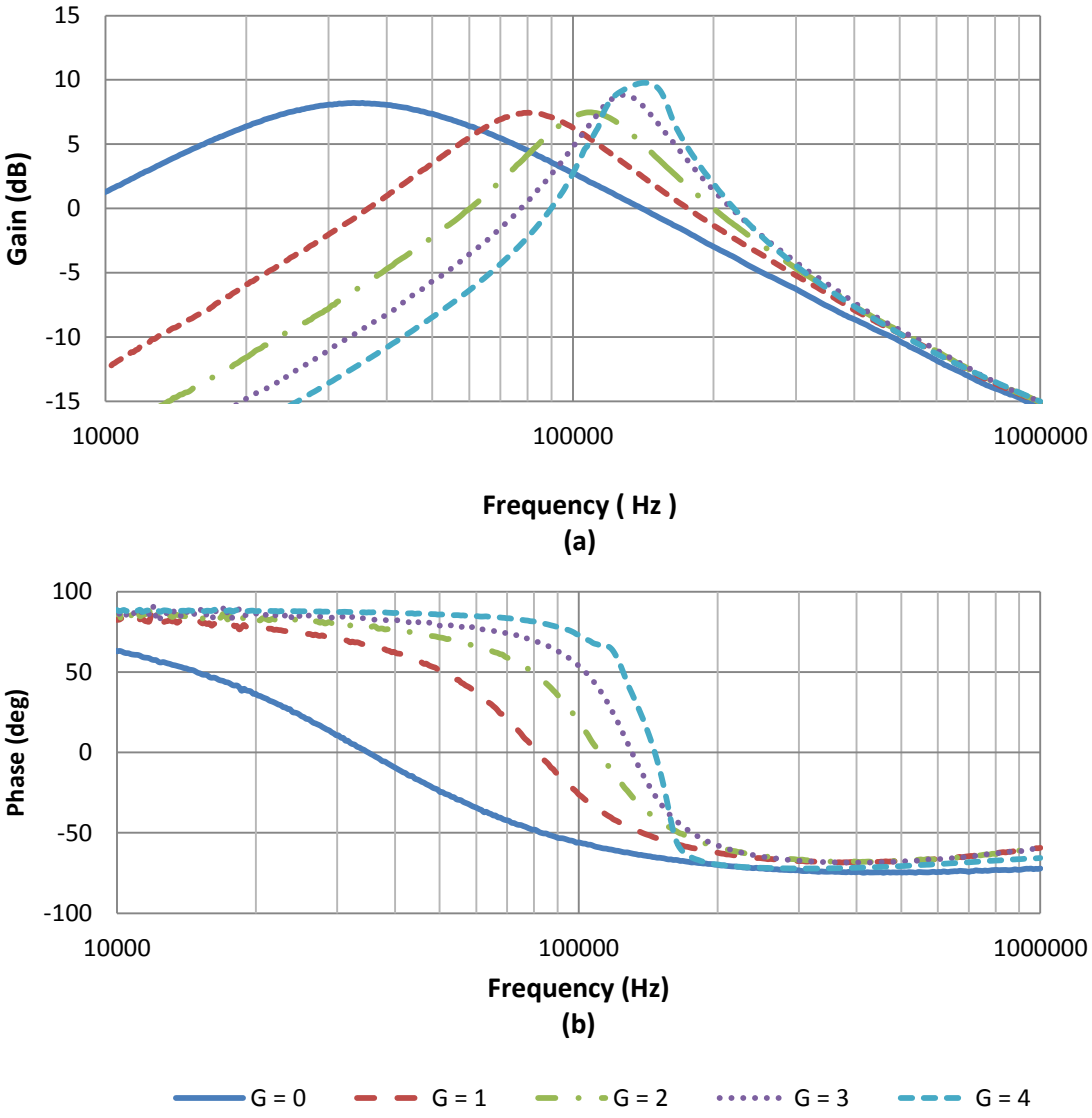

Fig. 13: The gain (a) and phase (b) frequency response of Fig.12

The BW of circuit Fig.12 should be theoretically constant while there is an error in the experimental results as shown in table 7. This error is around 10.7 % in the worst case and it is coming from the non-idealities of the amplifer used, which is in this case CFOA.

Fig.14 shows center frequency variation versus feedback amplifier gain

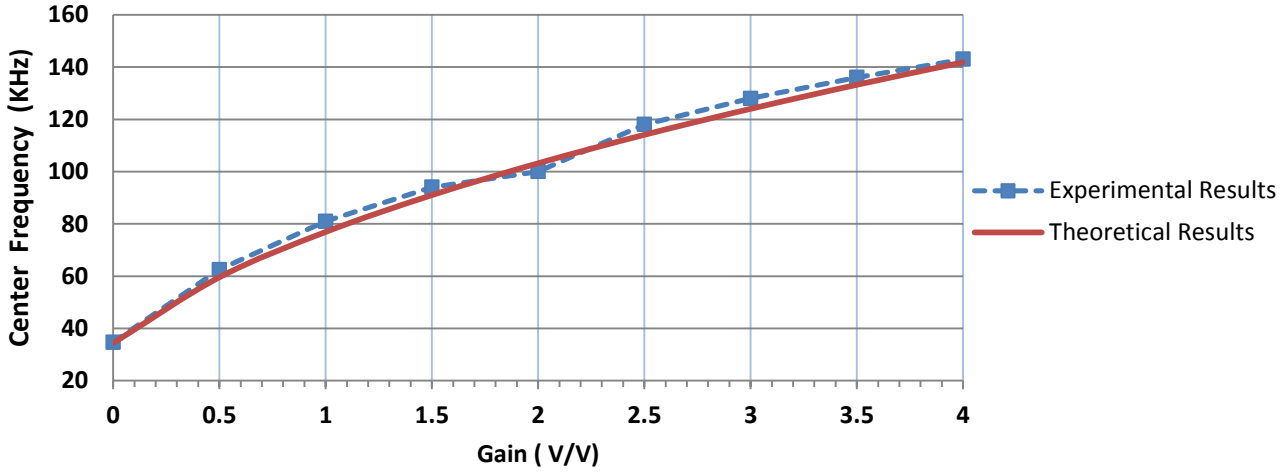

Fig. 14: Center frequency versus the gain

3.2 A New multi-feedback amplifiers band-pass shadow filter:

A number of feedback amplifers can be applied to the proposed bandpass shadow filter in Fig.9 so that the center frequency will be a function of feedback amplifers' gains.

Consider the mutiple input single output 2^{nd} order filter shown in Fig.15 with the transfer function in Eq.11 .When the input signal is fed to $V_{in,}$ a bandpass filtering function will be produced at the output provided that all the other inputs (V_1,V_2…V_n) are grounded. However, when the input signal is fed to one of the inputs: V_1 up to V_n , a low pass filtering function will be produced at the output provided that all the others inputs are grounded.

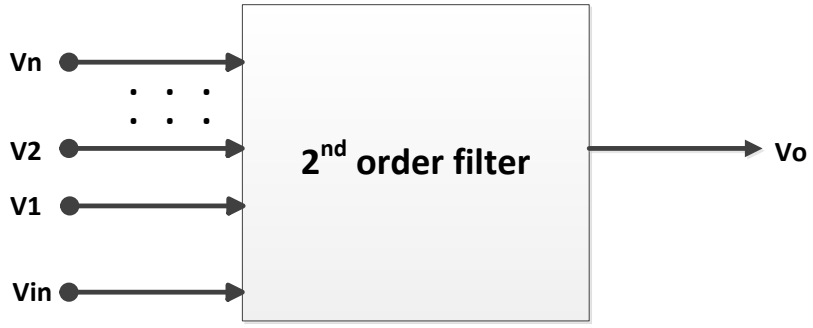

Fig. 15: Mutiple inputs single output filter

$$V_O = \frac{AsV_{in} + B_1V_1 + B_2V_2 \ldots B_nV_n}{as^2 + bs + 1} \qquad (11)$$

A new proposed multi-feedback amplifiers bandpass shadow filter can be obtained by connecting n number of feedback amplifers from the output to the inputs (V_1,V_2… V_n) while the input signal is fed to V_{in} as shown in Fig.16.

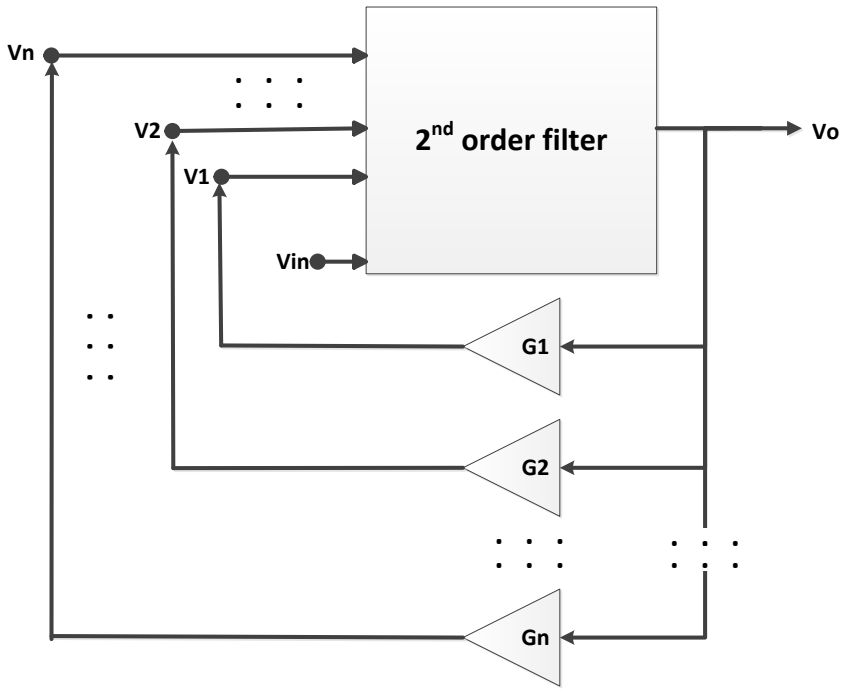

Fig. 16: Multi- feedback amplifiers bandpass shadow filter

Analysis:

Assuming a, b, A and B_i (i=1, 2,…n) are real positive:

$$V_O = \frac{AsV_{in} + G_1B_1V_o + G_2B_2V_o \ldots G_nB_nV_o}{as^2 + bs + 1} \tag{12}$$

➔ $$V_O\left[1 - \frac{G_1B_1 + G_2B_2 \ldots G_nB_n}{as^2 + bs + 1}\right] = \frac{AsV_{in}}{as^2 + bs + 1} \tag{13}$$

➔ $$V_O = \frac{AsV_{in}}{as^2 + bs + 1 - (G_1B_1 + G_2B_2 \ldots G_nB_n)} \tag{14}$$

➔ $$V_O = \frac{\frac{AsV_{in}}{1 - (G_1B_1 + G_2B_2 \ldots G_nB_n)}}{\frac{a}{1 - (G_1B_1 + G_2B_2 \ldots G_nB_n)}s^2 + \frac{b}{1 - (G_1B_1 + G_2B_2 \ldots G_nB_n)}s + 1} \tag{15}$$

Using eq.5, the filter characteristics are summarized in table 8.

Table 8: Filter characteristics of Fig.16

Center Frequency	***Bandwidth***	***Band pass Gain***
$f_O = \frac{1}{2\pi}\sqrt{\frac{1}{a}}\sqrt{1-(G_1B_1+G_2B_2\ldots G_nB_n)}$	$BW = \frac{b}{2\pi a}$	$G_{BPF} = \frac{Aa}{b}$

Now, the the center frequency of the shadow filter will be a function of the feedback amplifers' gain. The multi-feedback amplifers shadow filter can be used to get higher tuning range for the center frequency since as the number of feedback amplifiers increases, the tuning range of the center frequency increases. Also, it can be very useful in the fine tuning and course tuing for the center frequency.

3.2.1 Practical Implementation for the new proposed multi-feedback amplifiers band-pass shadow filter:

To verify the new proposed multi-feedback amplifiers bandpass shadow filter, a second order multi-inputs single outputs filter [12] is implemented as shown in Fig.17; where V_1,V_2 & V_3 produce a low pass filtering function in the output provided that all other inputs are grounded while the V_{in} produces a band pass filtering function at the output.

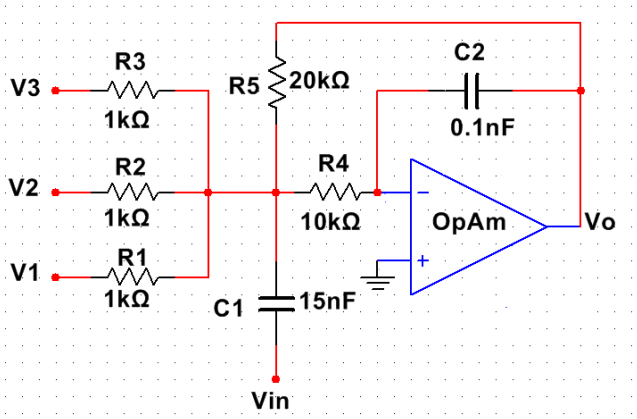

Fig. 17: Muti-inputs single output OpAm filter [12]

The transfer function of Fig.17 is:

$$V_O = \frac{-\frac{1}{C_2R_4}sV_{in} - \frac{1}{C_1C_2R_4R_1}V_1 - \frac{1}{C_1C_2R_4R_2}V_2 - \frac{1}{C_1C_2R_4R_3}V_3}{s^2 + s(\frac{1}{R_1}+\frac{1}{R_2}+\frac{1}{R_3}+\frac{1}{R_4}+\frac{1}{R_5})/C_1 + \frac{1}{C_1C_2R_4R_5}} \qquad (16)$$

The filter in Fig.17 is implemented with the corresponding components' value in the figure. To achieve a band pass filter, V_1,V_2 & V_3 set to ground and the input signal is fed to V_{in}. Table.9 shows the experiemental results of possible scenarios for feeding the input signal to circuit of Fig.17.

Table 9: The possible scenarios of input signal to circuit of Fig.17

	Type of Filter	Gain (V/V)	f_O (KHz)
Vin = input signal	BPF	4.7	**9.3 *KHz***
V_1, V_2 or V_3 = input signal	LPF	20	**9.3 *KHz***

To verify the multi-feedback amplifiers bandpass shadow filter's diagram which is proposed in Fig.16, a three current feedback amplifiers from the output to V_1,V_2 & V_3 are

applied for case n = 3 as shown in Fig.18, while for case n = 2; a two current feedback amplifiers from the output to V_1 & V_2 are applied as shown in Fig.19, and also for case n = 1, a single current feedback amplifier is applied from the output to V_1 as shown in Fig.20

The center frequency for the three cases of the shadow filter:

$$f_{O3} = f_O\sqrt{1-(G_1A_{LP1}+G_2A_{LP2}+G_3A_{LP3})} \quad ; \; n=3 \qquad (17)$$

$$f_{O2} = f_O\sqrt{1-(G_1A_{LP1}+G_2A_{LP2})} \quad ; \; n=2 \qquad (18)$$

$$f_{O1} = f_O\sqrt{1-(G_1A_{LP1})} \quad ; \; n=3 \qquad (19)$$

Where A_{LP1},A_{LP2} & A_{LP3} represent the DC gain of the low pass filters when the input signal is fed to one of the V_1,V_2 & V_3 and the other inputs are grounded including V_{in} as it is clear in Fig.17 and Eq.16

And G_1,G_2 & G_3 represent the gain of the current feedback amplifiers and they are tuned together from gain 0 V/V up to 1 V/V during the expreiement for the three cases $n = 1,2,3$ to compare the tuning range of the center frequency for these three cases..

In Fig.17 example, the DC gain of the three low pass filters are set to be identical

$$A_{LP1} = \frac{R_5}{R_1} = A_{LP2} = \frac{R_5}{R_2} = A_{LP3} = \frac{R_5}{R_3} = -20\ V/V \qquad (20)$$

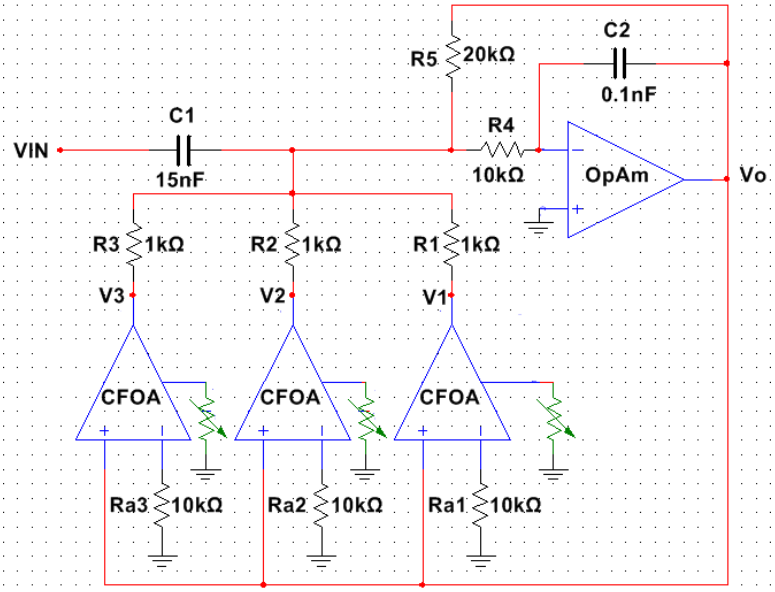

Fig. 18: triple feedback amplifier bandpass shadow filter (n = 3)

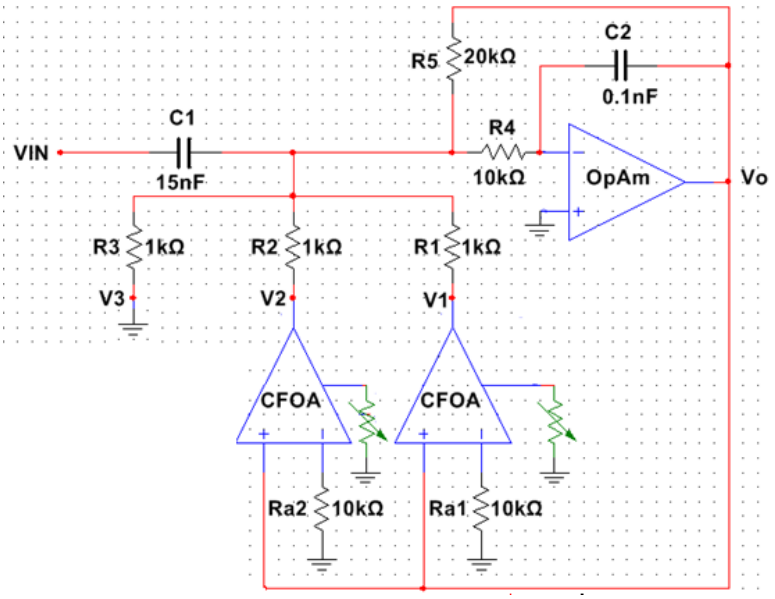

Fig. 19: double feedback amplifier bandpass shadow filter (n = 2)

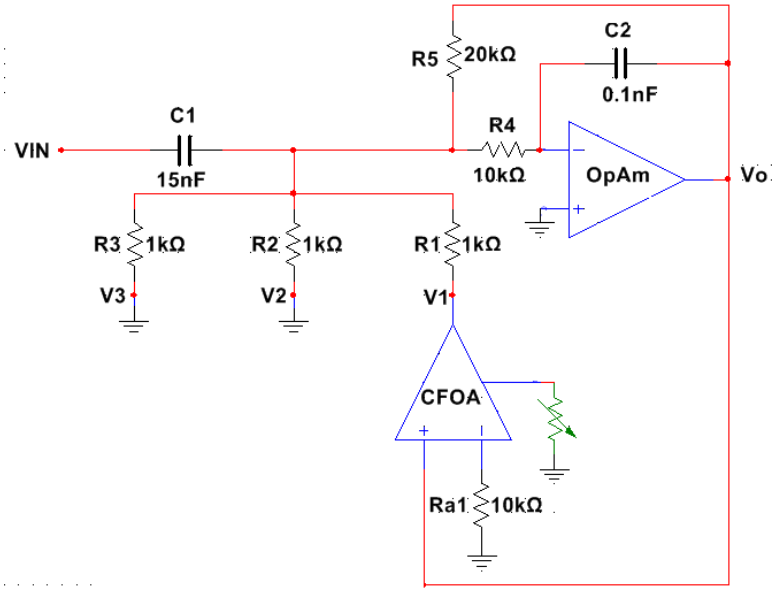

Fig. 20: single feedback amplifies bandpass shadow filter (n = 1)

The three circuits in Fig18, 19 and 20 are implemented and the amplifiers' gain are unified and set to be tuned from gain 0 V/V to gain 1 V/V to show the tuning range of the center frequency..

Fig. 21 shows the center frequency versus the feedback amplifiers' gain for different number of feedback amplifers banpass shadow filters

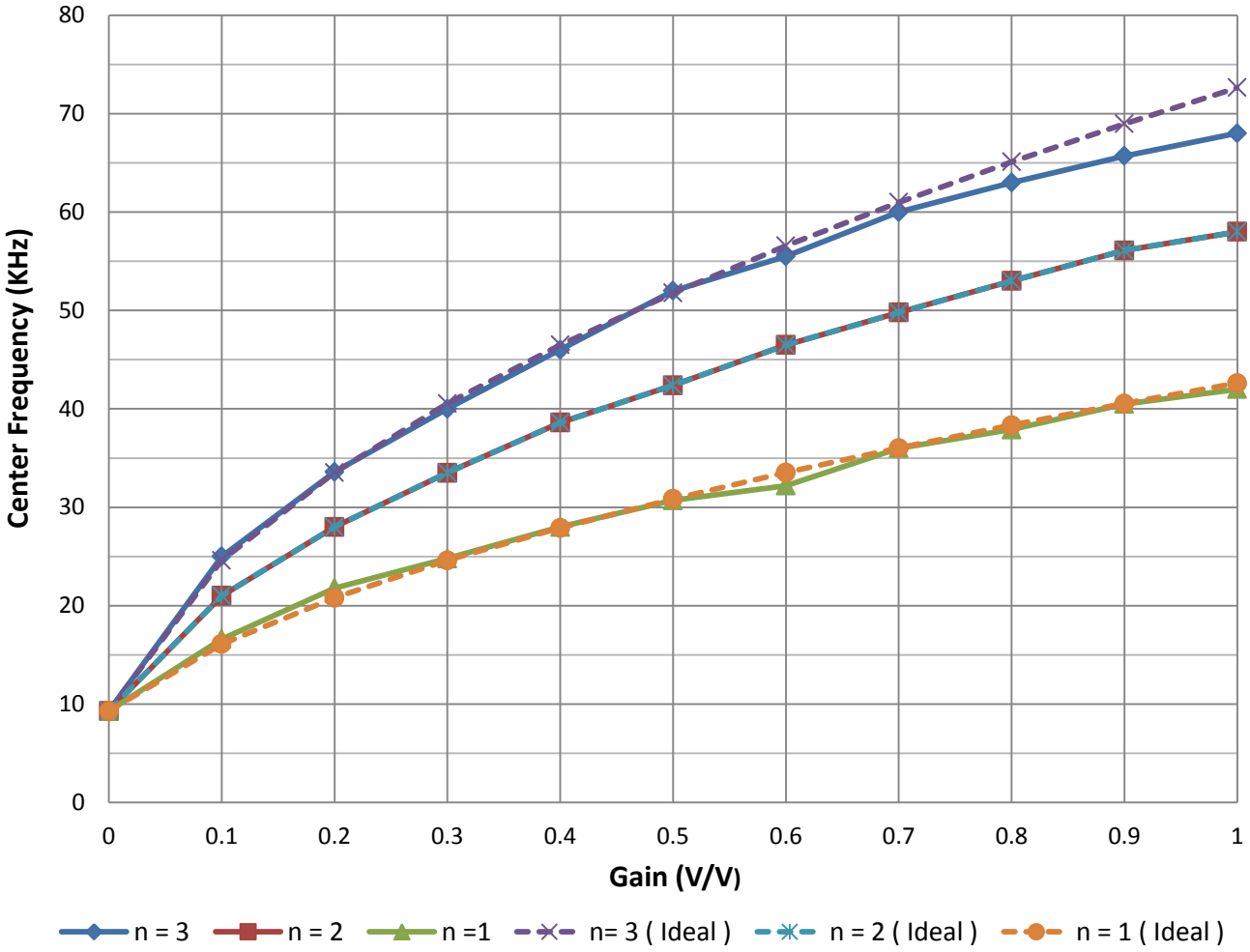

Fig. 21: The center frequency of the banpass shadow filters of Fig.18-20 versus the feedback amplifiers' gains

Fig21 shows the center frequency of the shadow filter versus the gain of the feedback amplifer. The error percentage does not exceed 8% especially when the center frequency excced 60 KHz. This error is due to the erro in the phase shift of the feedback amplifier and this error is resulted from the non ideality of used CFOA.

3.3 Tuning the bandwidth of the notch filter based on the shadow filter theory:

The idea of the shadow filtering can be extended to tuning the bandwidth of the notch filter.

Consider a second order dual input single output filter as shown in Fig.22 with the transfer function.

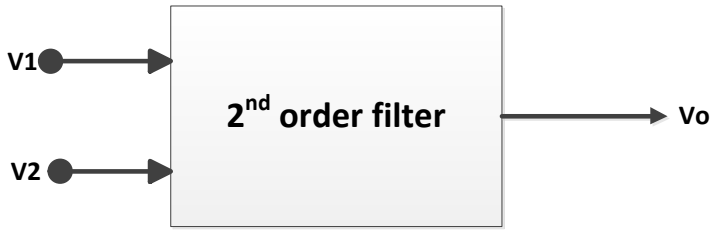

Fig. 22: Basic 2nd order filter

$$V_O = \frac{(As^2 + B)V_1 + CsV_2}{as^2 + bs + 1} \quad (21)$$

Assuming A, B,C, a and b are real positive, The filter characteristics is summarized in table 10:

Table 10 shows the filter parameters of Fig.22

Center Frequency	*Bandwidth*	*Notch Filter Gain (V_2=0)*	*Band Pass Gain (V_1=0)*
$fo = \frac{1}{2\pi}\sqrt{\frac{1}{a}}$	$BW = \frac{b}{2\pi a}$	$LF\ Gain = B$ $HF\ Gain = \frac{A}{a}$	$G_{BPF} = C\frac{a}{b}$

If the input signal is fed to V_1 and the output signal is amplified and fed to V_2 as in Fig.23, the output will be a notch filter such its bandwidth is controlled by the gain of the amplifier while the center frequency is fixed as shown in table 11.

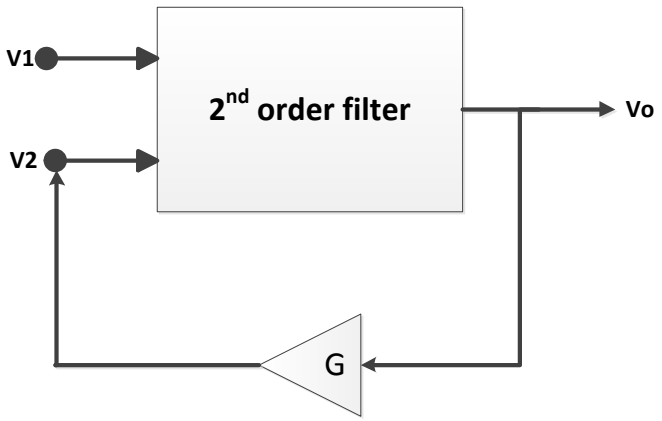

Fig. 23: Shadow notch filter

The new transfer function will be:

$$V_o = \frac{(As^2 + B)V_1}{as^2 + (b - GC)s + 1} \tag{22}$$

Table 11:The filter's parameters of Fig.23

Center Frequency	*Bandwidth*	*Notch filter Gain*
$fo = \frac{1}{2\pi}\sqrt{\frac{1}{a}}$	$BW = \frac{b - GC}{2\pi a}$	$LF\ Gain = B$ $HF\ Gain = \frac{A}{a}$

3.3.1 Practical Verification for the Proposed Notch Filter:

To verify the new scheme of the notch filter, a dual input single output CFOA filter is implemented. It is a modification version of the proposed circuit in [8] and shown in Fig.24

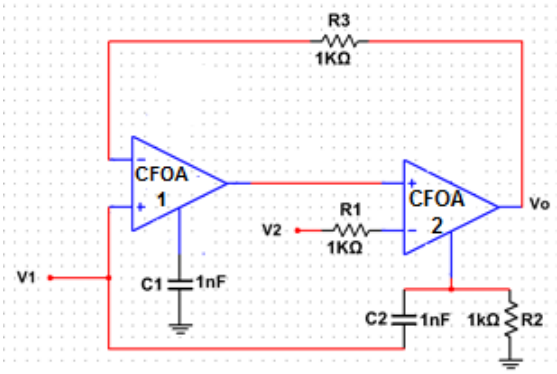

Fig. 24: DISO CFOA Filter [8]

The transfer function is:

$$V_o = \frac{\left(s^2 + \frac{1}{R_1 R_3 C_1 C_2}\right) V_1 \; - s\frac{1}{R_1 C_2} V_2}{s^2 \; + \; s\frac{1}{C_2 R_2} \; + \; \frac{1}{R_1 R_3 C_1 C_2}} \qquad ((23)$$

Fig.25 shows the gain and phase frequency response using NI ELVIS II+ breadboard where V_2 is grounded in order to get notch response at the output.

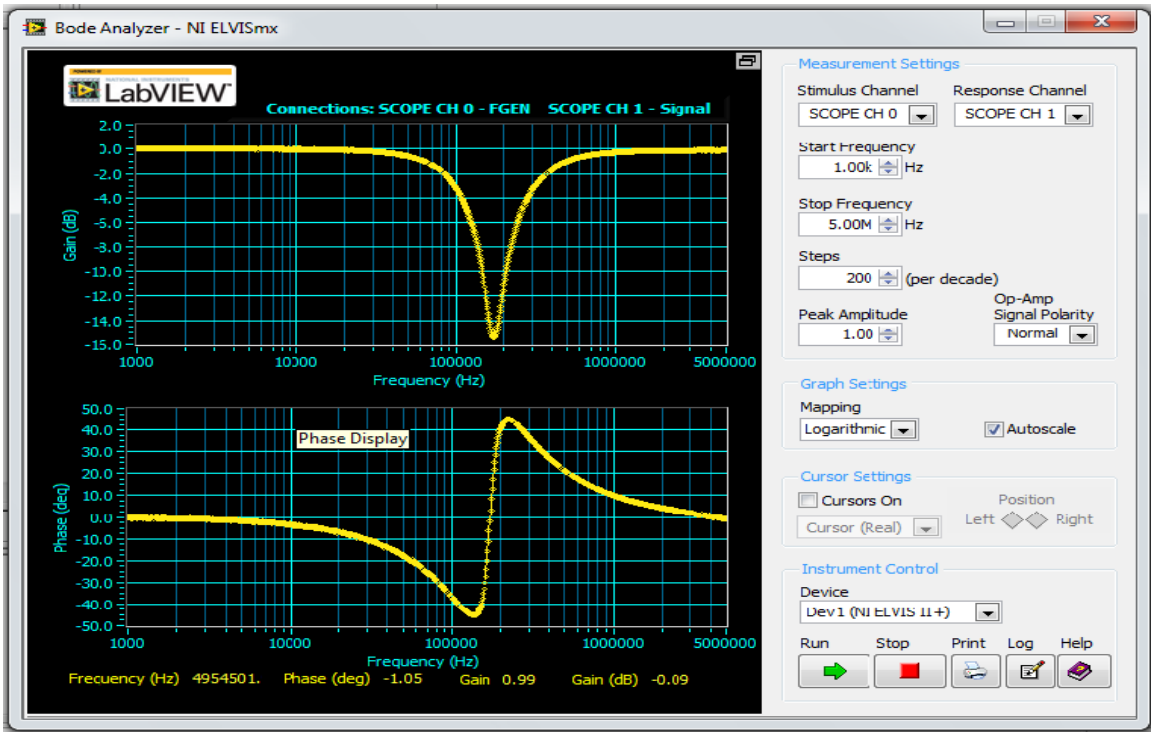

Fig. 25: gain and phase frequency response of Fig.24 using NI ELVIS II+

Table 12: The theoretical and experimental results of Fig.24

	Center Frequency	***Bandwidth***	***The Pass Band Gain***
Theoretically	***159.1 KHz***	***159.1 KHz***	**1**
Experimentally	***173 KHz***	***191 KHz***	**1**

After taking the experiemental measurements of notch filter,a feedback amplifier is applied from the output to the V_2 as shown in Fig.26:

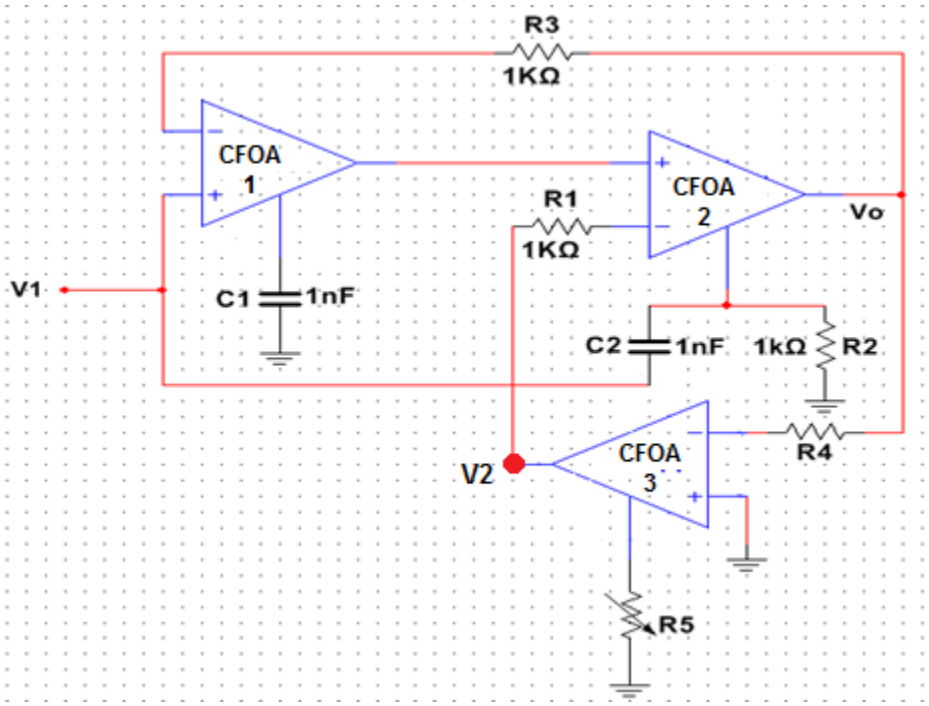

Fig. 26: Shadow notch filter

The new transfer function of the notch filter is:

$$V_O = \frac{\left(s^2 + \frac{1}{R_1 R_3 C_1 C_2}\right) V_1}{s^2 + s\left(\frac{1}{C_2 R_2} + G\frac{1}{R_1 C_2}\right) + \frac{1}{R1R3C1C2}} \qquad ((24)$$

So, the bandwidth of the notch filter is controlled by the gain of the feedback amplifer where $G = -R_5/R_4$. While the center frequency of the notch filter is fixed.

The circuit in Fig.26 is implemented and tested in the lab under several values of the feedback voltage amplifier gain (-0.2,-0.4,-0.6,-0.8). Table13 shows the theoretical and experimental values of the bandwidth for the notch filter in Fig.26.

Table 13: Experimental and Theoretical results of the notch filter of Fig.26

G	Theoretical Values	Experimental Values
0	160 KHz	191 KHz
-0.2	127 KHz	174 KHz
-0.4	95 KHz	134 KHz
-0.6	63 KHz	97 KHz
-0.8	32 KHz	50 KHz

The difference between the theoretical and the experimental values is coming from the non-idealities of the feedback amplifier CFOA3 (Fig.26). The feedback amplifer is expected to produce amplifed output signal with 180^{o} phase shift. Since the center frequency of notch filter is relatively high around 170 KHz ,so there is significant error in the phase of the feedback amplifer which contribues in disturbing the bandwidth of the notch filter.

Fig.27 shows the gain frequency response of Fig.26

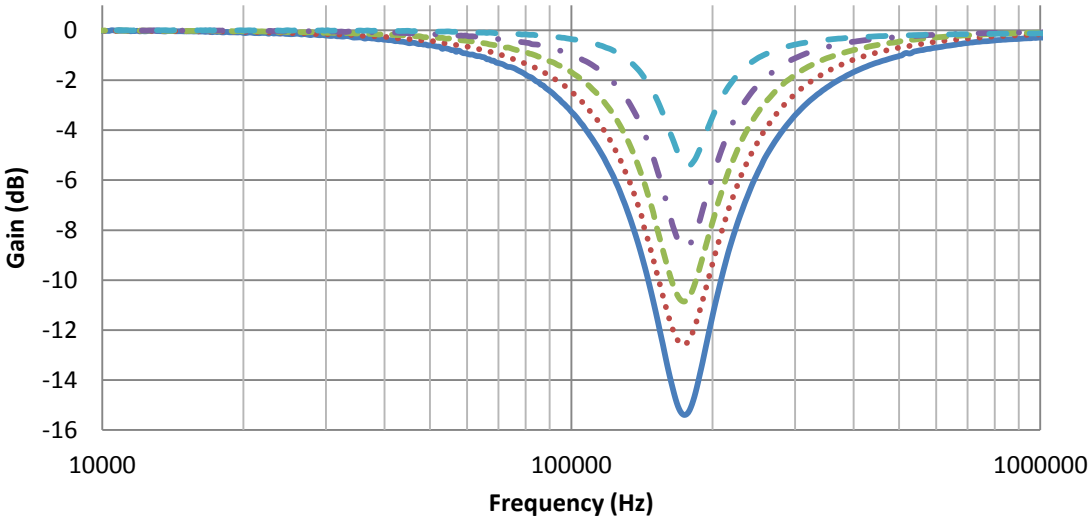

Fig. 27: Gain and frequency response of the notch filter of Fig.26

3.4 Tuning the center frequency of the notch filter based on the shadow filter theory:

The center frequency of notch filter can be tuned using the concept of the shadow filter theory. Usually, any notch filter can be obtained from summing the low pass filter and the high pass filter as shown in Fig.28.

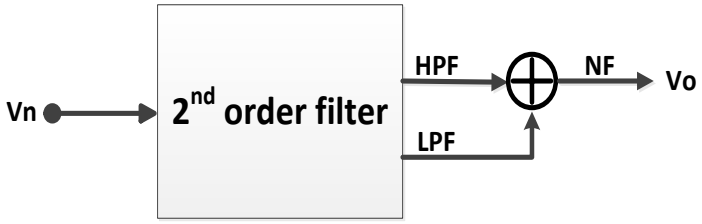

Fig. 28: Notch Filter Diagram

Assuming A, B,C, a and b are real positive:

$$V_O = \frac{(A + Bs^2)V_n}{as^2 + bs + 1} \tag{25}$$

Table 14: The center frequency and the gain of Fig.28

Center Frequency	*Notch Filter Gains*
$fo = \frac{1}{2\pi}\sqrt{\frac{1}{a}}$	$DC\ Gain = A, \qquad HF\ Gain = B/a$

If the low pass output is amplified and fed to the input with a summing circuit, the center frequency of the high pass output and the low pass output will be modified to $f_{OG} = f_O\sqrt{1 - GA_{LP}}$ (refer to [1] and Eq.12 -15). However, the DC gain of the low pass output will be reduced by a factor of $\frac{1}{1-GA_{LP}}$ while the high pass gain will stay constant. So, the DC gain should be compensated by an amplifier which has a gain of $(1 - GA_{LP})$ so that the high pass output and the amplified low pass output can be summed to obtain a

notch filter where the center frequency is controlled by the gain of the external amplifier as shown in Fig.29.

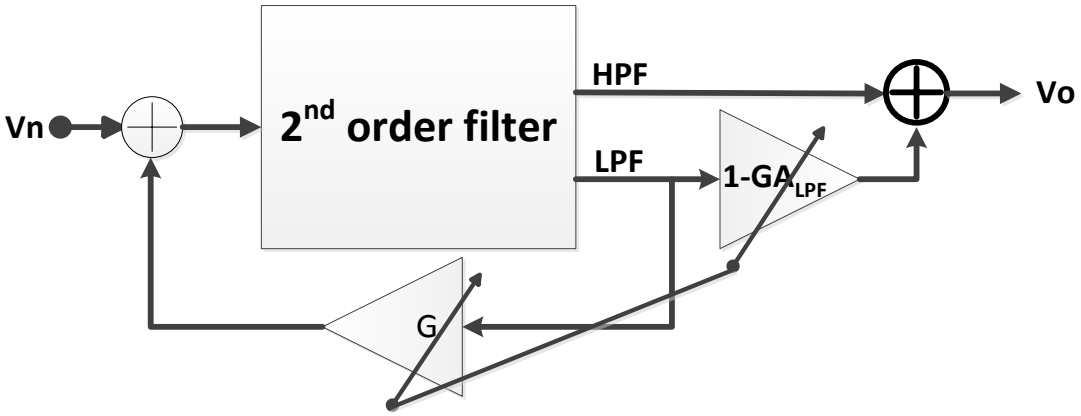

Fig. 29: Shadow notch filter

The new transfer function of Fig. 29 will be:

$$V_O = \frac{(\,Bs^2 + A(1 - GA_{LPF})\,)V_n}{as^2 \;+\; bs \;+\; 1 - GA_{LPF}} \tag{26}$$

Table 15: The center frequency and the gain of Fig.29

Center Frequency	*Notch filter Gain*
$fo = \frac{1}{2\pi}\sqrt{\frac{1}{a}}\sqrt{1 - GA_{LPF}}$	$DC\ Gain = A/a\,, \quad HF\ Gain = B/a$

3.4.1 Practical Verification for proposed shadow Notch Filter:

To verify the shadow notch filter scheme proposed in Fig.29, a single input multi output CFOA filter, which was proposed in [11] is implemented as shown in Fig.30

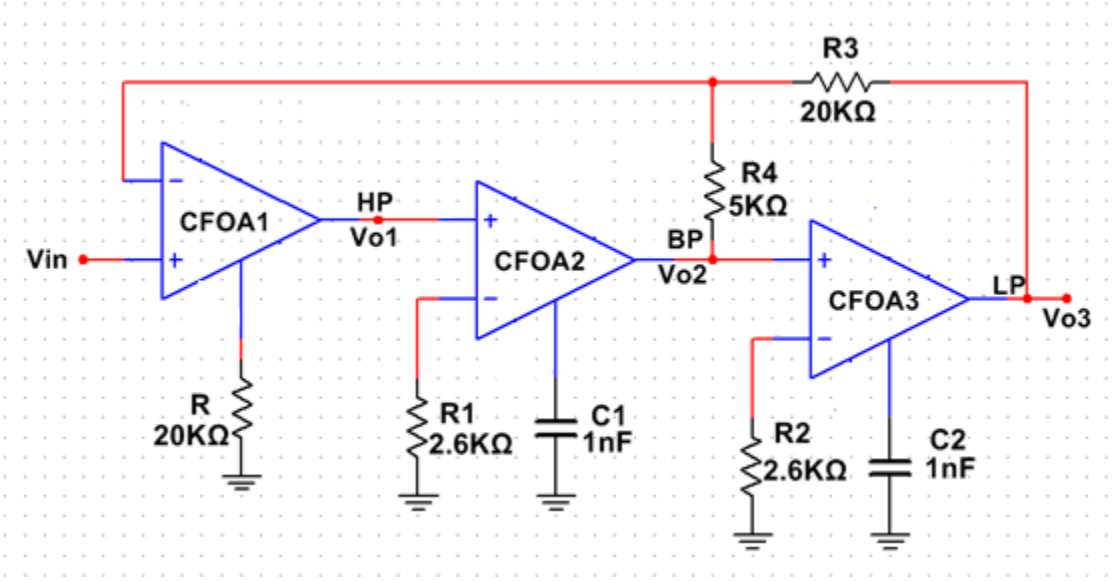

Fig. 30: Single input multi-outputs CFOA filter [11]

The transfer functions of the three outputs V_{O1}, V_{O2} & V_{O3} are:

$$V_{o1} = \frac{\frac{R(R_3+R_4)}{R_4R_3}s^2\ V_{in}}{s^2 + s\frac{R}{C_1R_1R_4} + \frac{R}{R_1R_2R_3C_1C_2}} \qquad ((27)$$

$$V_{o2} = \frac{\frac{R(R_3+R_4)}{R_1C_1R_3R_4}s\ V_{in}}{s^2 + s\frac{R}{C_1R_1R_4} + \frac{R}{R_1R_2R_3C_1C_2}} \qquad ((28)$$

$$V_{o3} = \frac{\left(\frac{R(R_3+R_4)}{R_1R_2R_3R_4C_1C_2}\right)V_1}{s^2 + s\frac{R}{C_1R_1R_4} + \frac{R}{R_1R_2R_3C_1C_2}} \qquad ((29)$$

Based on equations: 27-29, the notch filter can be obtained by summing the low pass output with high pass output as shown in Fig.31

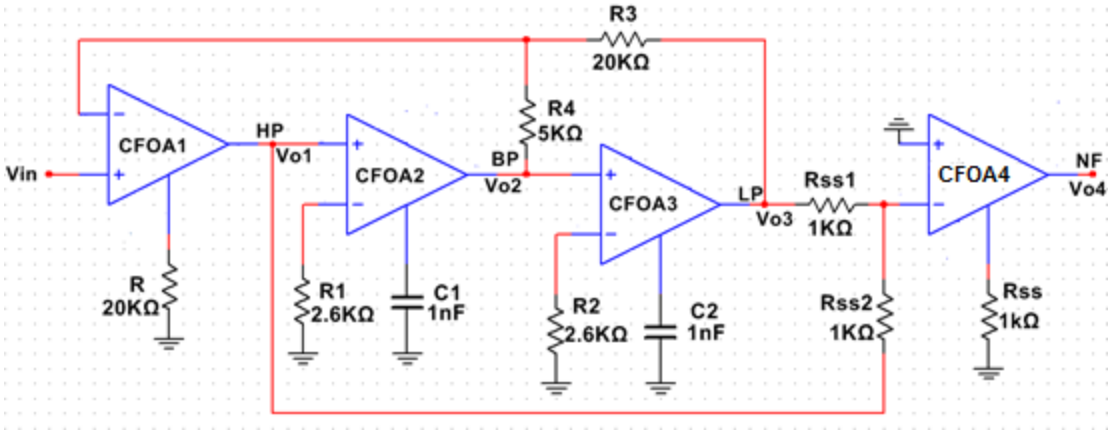

Fig. 31: Single inputs multi outputs

Fig.32 shows the gain and phase frequency response for V_{O4} of Fig.31 which is a notch filter. The experimental data was taken using NI ELVIS II+ breadboard.

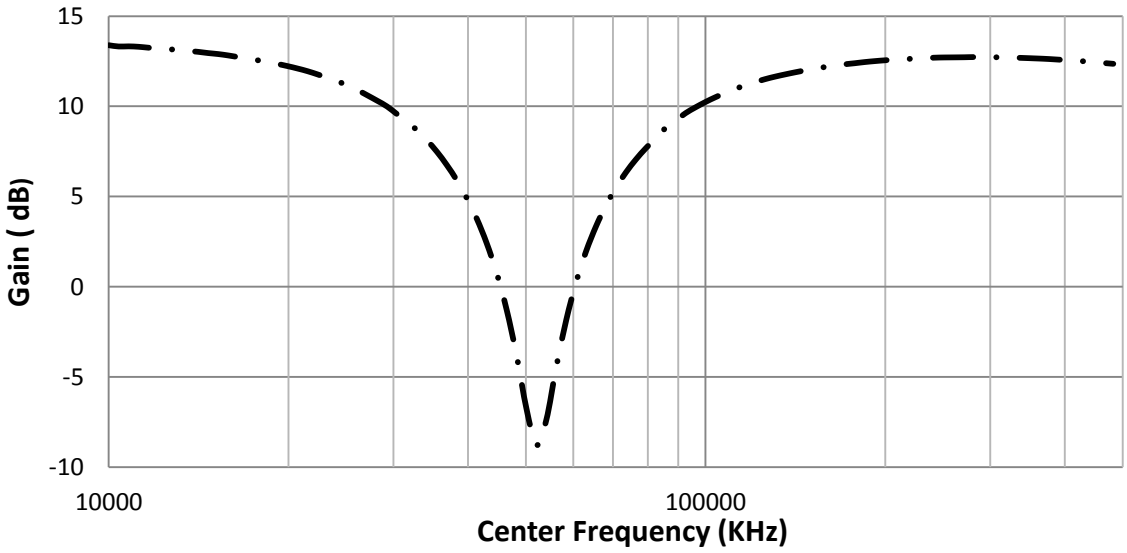

Fig. 32: Gain frequency response for the notch filter of Fig.30

Table 14 : The gain and the center frequency for notch filter of Fig.31

Center frequency (KHz)	DC Gain (dB)	High frequency Gain (dB)
53 KHz	13.3	13

In order to match the shadow notch filter proposed in Fig.29, a feedback amplifier is introduced from V_{O3} (low pass output) to the summing circuit at the input. In addition to that, another amplifier with gain $(1 + GA_{LPF})$ is introduced from V_{O3} the summing circuit at the output to compensate for the DC gain reduction of the low pass filter due to the feedback amplifier as shown in Fig.33

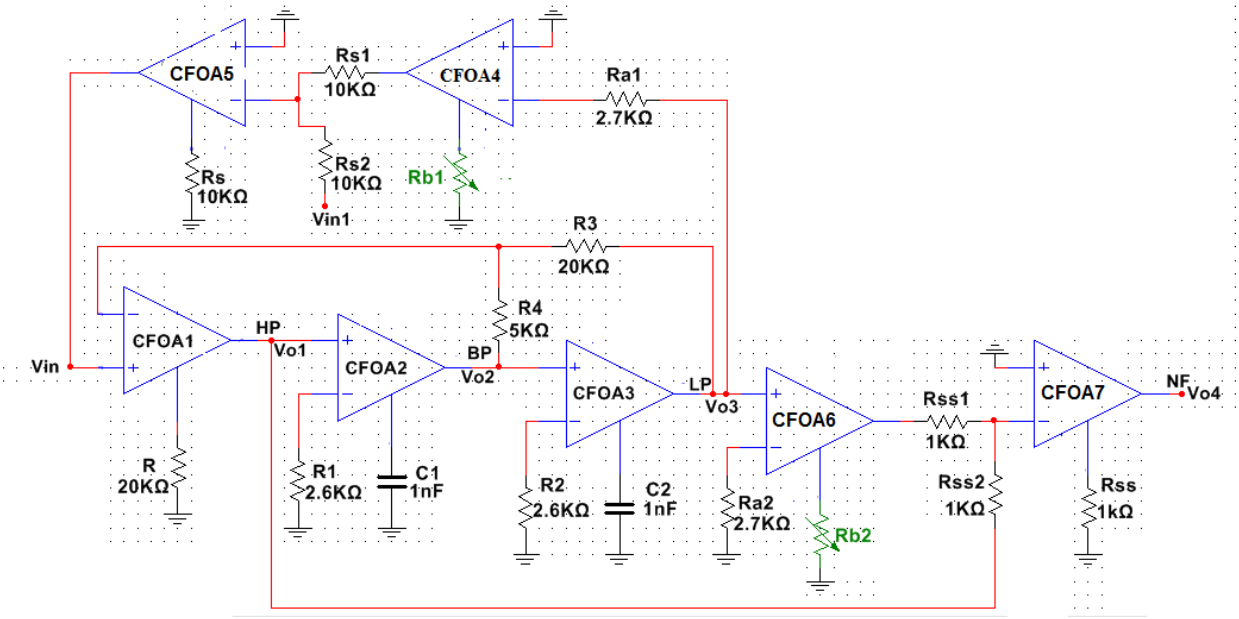

Fig. 33: Shadow notch fitler based on CFOA

The transfer function of Fig.33 is:

$$V_{O4} = \frac{\left(\frac{R(R_3+R_4)}{R_4R_3}s^2 + \frac{R(R_3+R_4)(1-A_{DC}G)}{R_1R_2R_3R_4C_1C_2}\right) V_{in1}}{s^2 + s\frac{R}{C_1R_1R_4} + \frac{R}{R_1R_2R_3C_1C_2}(1-A_{DC}G)} \qquad ((30)$$

Where the A_{DC} represents the DC gain of the low pass filter V_{O3} given by $A_{DC} = (R_3 + R_4)/R_4 = 5$. While **G** represents the gain of the feedback amplifier (CFOA4) given by $\mathbf{R_{b1}/R_{a1}}$.In Fig.33; CFOA5 and CFOA7 are summing amplifiers while CFOA6 represents the compensation amplifier and CFOA4 is the feedback amplifier.

The circuit in Fig.33 is implemented experimentally and tested for several values of feedback's gain (-0.2, -0.6, -1.6, -3 and -5) where the gain of the compensation amplifier (CFOA6) is modified accordingly to maintain equal DC and HF gains for different responses. Fig.34 shows the gain frequency response for the circuit of Fig.33. There is a small error in the center frequency due the non-idealities of the CFOA. Additionally, when the gain is $5V/V$, the error is around 10% and it is resulted the mismatch between the feedback amplifier and the compensation amplifier.

Table 15:The gain and the center frequency for notch filter of Fig.33

$G\ (V/V)$	$1-A_{DC}G\ \ (V/V)$	$Experimental\ f_O\ (KHz)$	$Theoretical\ f_O\ (KHz)$
0	0	52	53
-0.2	2	76	75
-0.6	4	110	106
-1.6	9	161	159
-3	16	207	212
-5	26	237	262

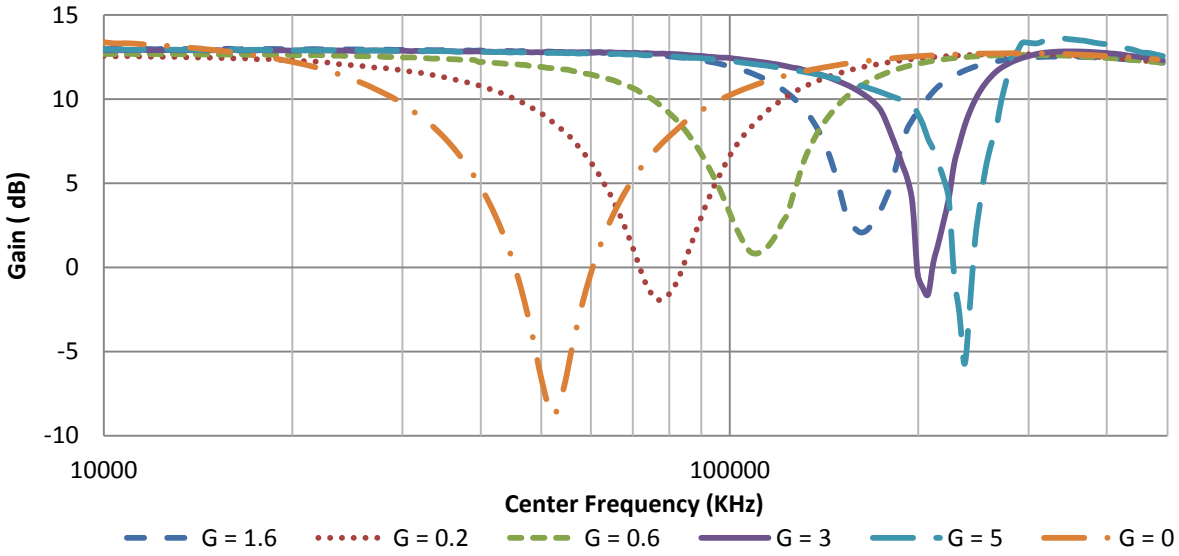

Fig. 34: The magnitude response of the notch filter of Fig.33

3.5 Tuning the Bandwidth of the Band-pass Shadow Filter:

In the proposed scheme of Fig.9, the center frequency of the bandpass filter is tuned by the amplifier gain without disturbing the bandwidth. Consider a multi input single output filter as in Fig.35 with the transfer function.

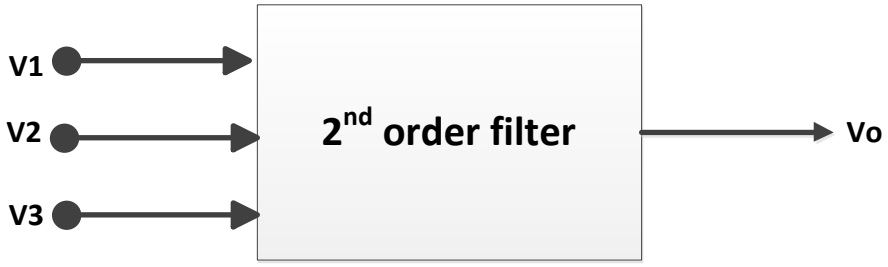

Fig. 35: MISO Filter

$$V_O = \frac{AsV_1 + BsV_2 + CV_3}{as^2 + bs + 1} \quad (31)$$

- Bandpass filter will be realized if $V_1 = V_{IN}$ and $V_2 = V_3 = 0$.
- Another bandpass filter will be realized if $V_2 = V_{IN}$ and $V_2 = V_3 = 0$.
- Low pass filter will be realized if $V_3 = V_{IN}$ and $V_2 = V_1 = 0$.

If the output signal is amplified by two amplifiers with gain G1 and G2, and they are fed to V_2 and V_3 as in Fig.36. The resulting filter will be a bandpass filter where its bandwidth and center frequency is independently controlled by these two amplifiers as it is clear in the corresponding transfer function.

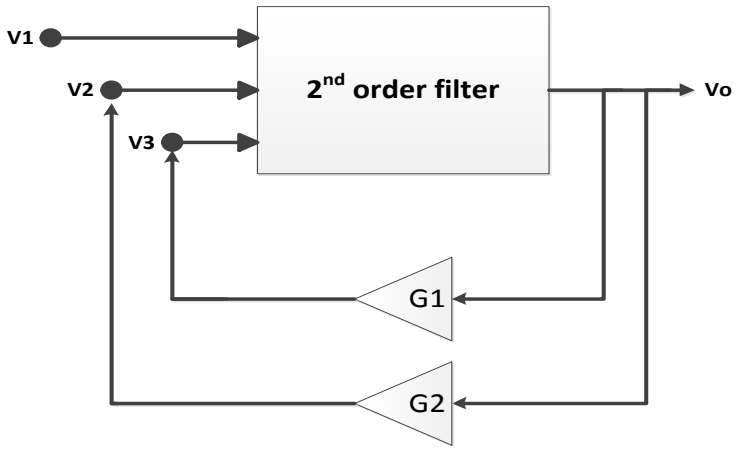

Fig. 36: Shadow band-pass filter with controllable bandwidth

The transfer function of the new filter is:

$$V_O = \frac{\frac{A}{1-G_2C}\, s\, V_1}{\frac{a}{1-G_1C}s^2 \quad + \quad \frac{b-G_2B}{(1-G_1C)}\, s \quad + \quad 1} \tag{32}$$

Center Frequency	***Bandwidth***	***Band pass Gain***
$\boldsymbol{f_O = \frac{1}{2\pi}\sqrt{\frac{1}{a}\sqrt{1-G_1C}}}$	$\boldsymbol{BW = \frac{b-G_2B}{2\pi a}}$	$\boldsymbol{G_{BPF} = Aa/(b-G_1B)}$

By this approach, the center frequency and bandwidth can be orthogonally controllable by G_1 and G_2, so it can be used for filters that does not enjoy orthogonal tuning.

3.5.1 Practical verification for tuning BW and f_O of the shadow filter:

Consider the circuit in Fig.37, proposed in [9], which has three inputs and single output with the transfer function.

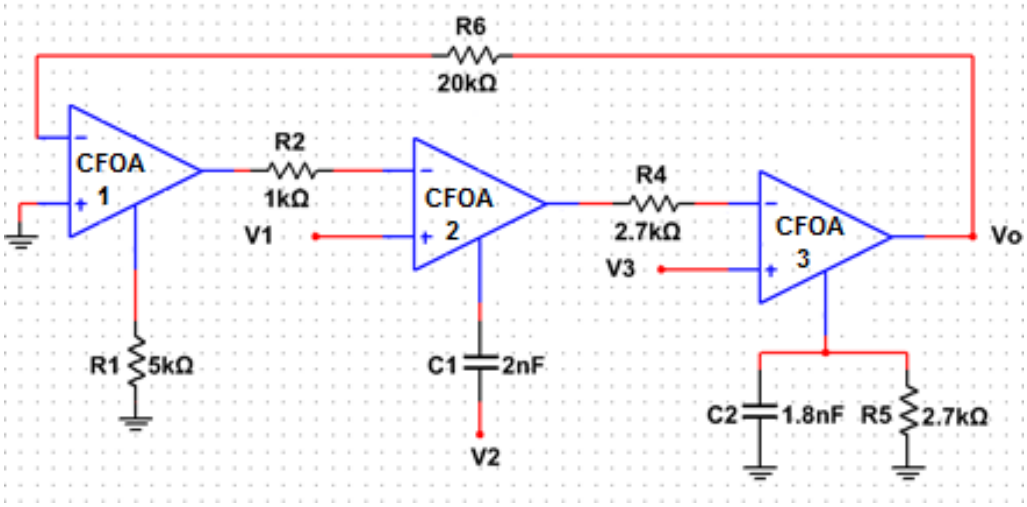

Fig. 37: Multi-inputs single outputs CFOA filter [9]

$$V_O = \frac{-\frac{1}{R_2R_4C_1C_2}V_1 - s\frac{1}{R_4C_2}V_2 + s\frac{1}{R_4C_2}V_3}{s^2 + s\frac{1}{C_2R_5} + \frac{R_1}{R_2R_4R_6C_1C_2}} \qquad (33)$$

The filter in Fig.37 is implemented in the NI ELVIS II+ breadboard. The inputs V_1 and V_2 set to the ground in order to realize band-pass filter. Table.16 illustrates the theoretical and experimental results.

Table 16: Theoretical and Experimental results of Fig.37

	Theoretical results	Experimental results
Center Frequency	25.8 KHz	26.2 KHz
Bandwidth	32.7KHz	35 KHz
Band-pass Gain	1	0.93

Applying two feedback amplifiers from the output to V_1 and V_2 as it is illustrated in Fig.38

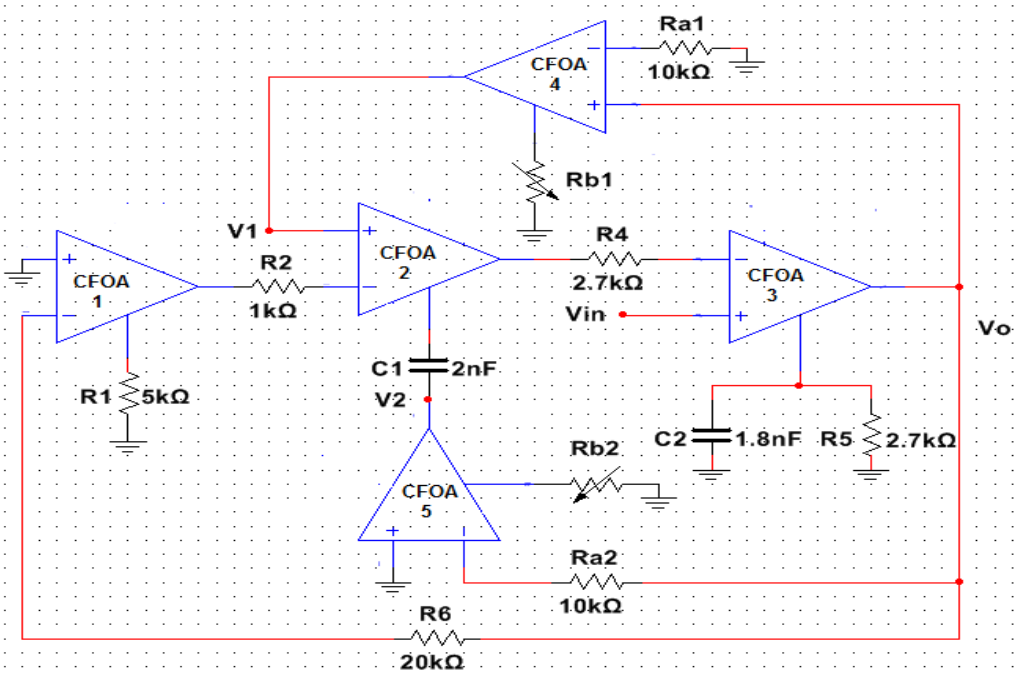

Fig. 38: Shadow CFOA band-pass filter with controlable bandwidth

The transfer function of Fig.38 where R_5=R_4=R is:

$$V_O = \frac{s\frac{1}{R_4C_2}V_3}{s^2 + s\frac{1}{C_2R}(1-B) + \frac{R_1}{R_2R_4R_6C_1C_2}(1+(\frac{R_6}{R_1})A)} \qquad (34)$$

A and B represent the feedback gains where $A = R_{b1}/R_{a1}$ and $B = -R_{b2}/R_{a2}$. Now, the bandwidth and center frequency can be independently controlled by A and B. This band-pass filter is tested for several values of A and B where R_6/R_1= 4. Table 17 shows the experimental and theoretical results. The error in the experimental results is due the significant error in the phase shift of the two feedback amplifers which contribues in disturbing the gain and the bandwidth, where the phase shift error is due to the non-idealities of the CFOA. The results are summarized in Table17 and Fig.39

Table 17: Summary for the experiemental and theoretical results of Fig.38

A	B	$f_{OThoeretical}$	f_{OExp}	$BW_{Thoeretical}$	BW_{Exp}	$G_{BPF\ Theoretical}$	$G_{BPF\ EXP}$
0	Zero	25.8	26 KHz	32.7 KHz	35 KHz	1	0.93
	-0.25			24.5 KHz	27 KHz	1.3	1.3
	-0.5			16 KHz	18 KHz	2	1.8
1	Zero	57.7	58 KHz	32.7 KHz	40 KHz	1	0.81
	0.25			24.5 KHz	36 KHz	1.3	0.95
	0.5			16 KHz	28 KHz	2	1.3
4	Zero	106.4	104 KHz	32.7 KHz	33 KHz	1	1.1
	0.25			24.5 KHz	22 KHz	1.3	2.2
	0.5			16 KHz	10 KHz	2	4.4

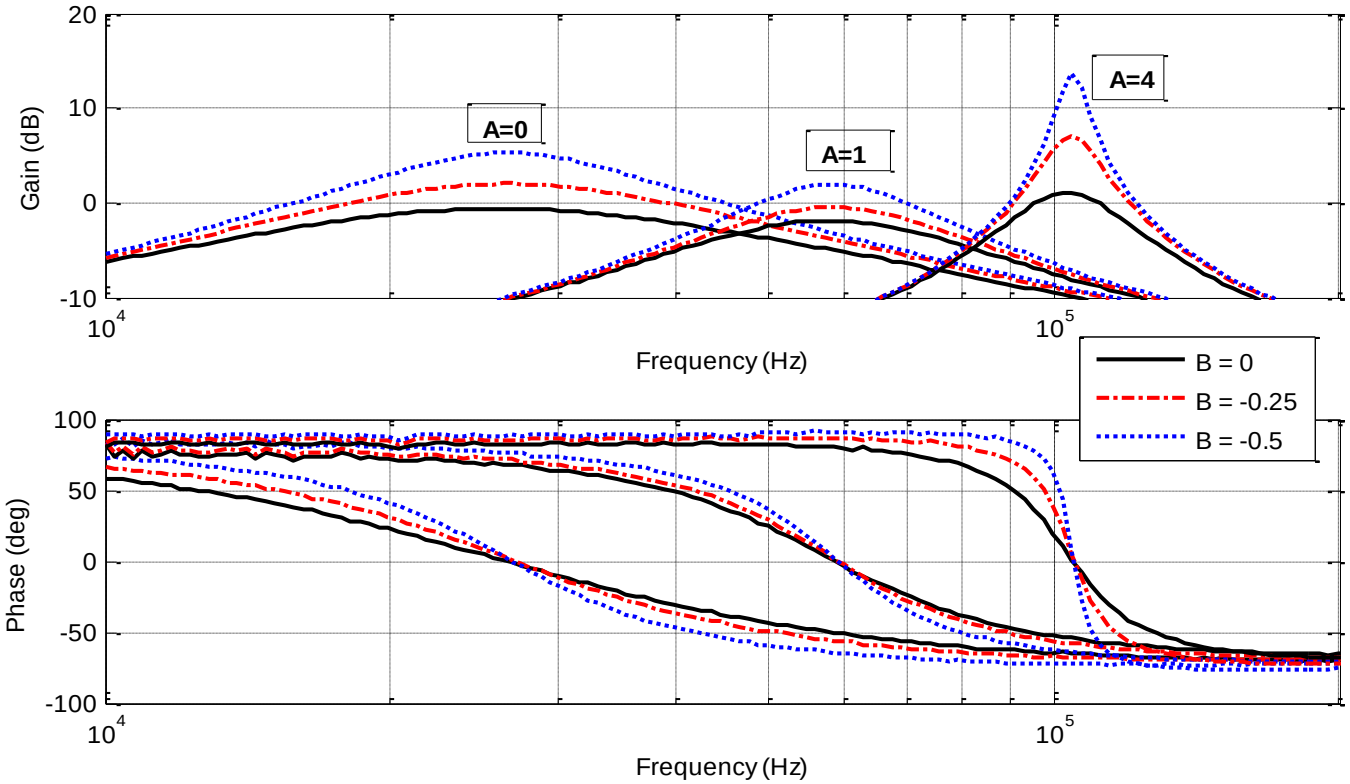

Fig. 39: Gain and Phase frequency response for mutiple of A and B

3.6 Tuning the Quality Factor and the Center Frequency of the High Pass Filter:

Consider the block diagram shown in Fig.40 with the corresponding transfer function in Eq.35:

Fig. 40: MISO Filter

$$V_O = \frac{As^2V_1 + BsV2 + CV_3}{as^2 + bs + 1} \tag{35}$$

- High-Pass filter will be realized if $V_1 = V_{IN}$ and $V_2 = V_3 = 0$.
- Band-pass filter will be realized if $V_2 = V_{IN}$ and $V_1 = V_3 = 0$.
- Low-pass filter will be realized if $V_3 = V_{IN}$ and $V_2 = V_1 = 0$.

Fig.41 shows a block diagram for a high pass filter where the quality factor *Q* and the center frequency *fo* is independently controlled by the two external amplifiers G_1 and G_2 as it is illustrated in Eq.36

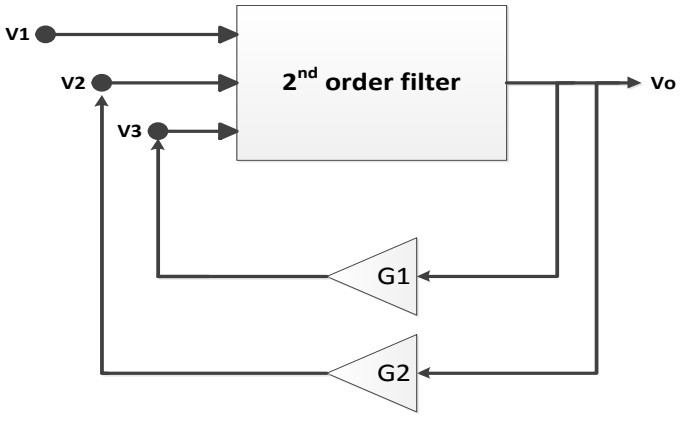

Fig. 41: Shadow High Pass Filter

$$V_O = \frac{A\frac{s^2}{1-G_1C}\,V_1}{\frac{as^2}{1-G_1C} + \frac{b-G_2B}{(1-G_1C)}\,s + 1} \quad (36)$$

Table 18: Shadow High Pass Parameters

Center Frequency	*Quality Factor*	*High pass Gain*
$\boldsymbol{fo = \frac{1}{2\pi}\sqrt{\frac{1}{a}\sqrt{1-G_1C}}}$	$\boldsymbol{Q = \frac{\sqrt{\frac{1}{a}\sqrt{1-G_1C}}}{\frac{b-G_2B}{a}}}$	$\boldsymbol{G_{HPF} = A/a}$

Table18 shows the expression of the center frequency and the quality factor of the high pass filter. Tuning the amplifier G_1, will tune the center frequency of the high pass filter and accordingly, the quality factor will be changed. So the amplifier G_2 can be used to have a control over the quality factor of the high pass filter.

3.6.1 Practical verification for tuning f_O and Q of the High Pass Filter:

The practical verification for the shadow high pass filter in Fig.41 is divided into two cases:

A. **Case#1**: G_1 is used to tune the center frequency of the high pass filter while G_2 is set to zero.

B. **Case#2**: G_1 is used to tune the center frequency of the high pass filter while G_2 is used to maintain the quality factor to be $1/\sqrt{2}$ to achieve a high pass filter with flat response.

A. Case#1:

Consider the circuit in Fig.42, proposed in [8], which has two inputs and single output with the transfer function given by:

$$V_O = \frac{-\frac{1}{R_1R_4C_1C_2}V_1 - s\frac{1}{R_1C_2}V_2 + s^2V_3}{s^2 + s\frac{1}{C_2R_2} + \frac{1}{R_1R_3C_1C_2}} \quad (37)$$

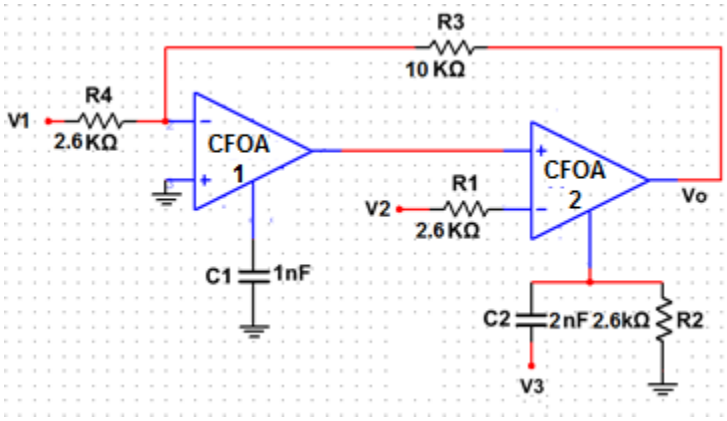

Fig. 42: DISO CFOA Filter [8]

The filter in Fig.42 is implemented in the NI ELVIS II+ breadboard. The inputs V_1 and V_2 set to the ground in order to realize high-pass filter. Fig.43 shows the gain and phase frequency response. Table.19 summarizes the results.

Table 19: Theoretical and Experimental Results of Fig42

	Theoretical result	Experimental result
fo	22 KHz	23.3 KHz
Quality factor	0.721	0.7
G_{HPF}	1	1

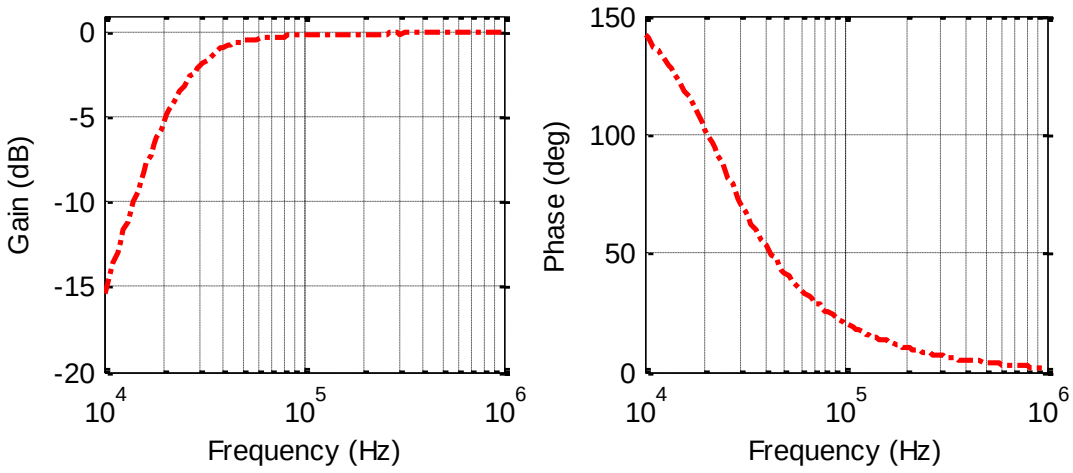

Fig. 43: Gain and Phase frequency response of Fig.42

The two feedback amplifiers are applied from the output to V_2 and V_3 to satisfy the block diagram of Fig.41 as it is illustrated in Fig.44.

The amplifiers CFOA3 provides G_1 while G_2 is provided by CFOA4.

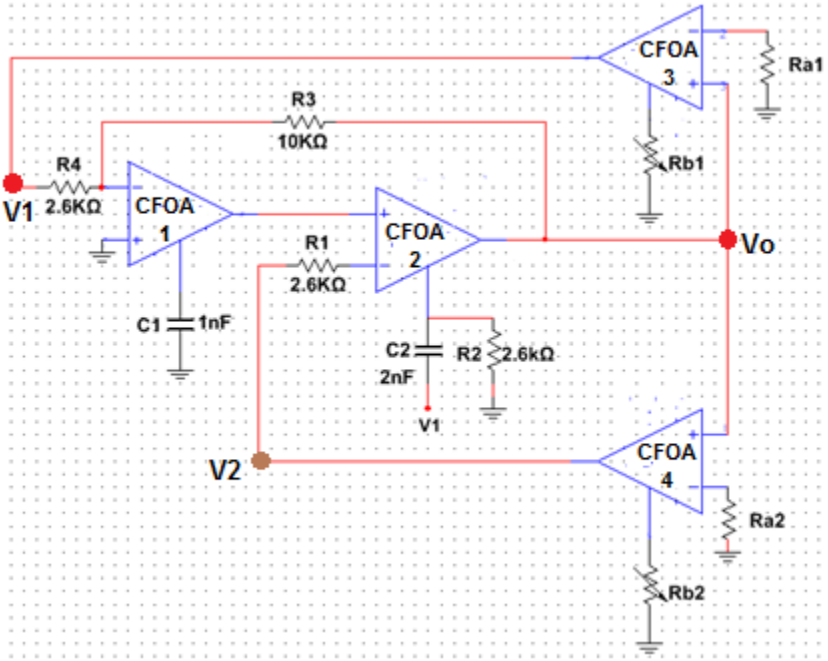

Fig. 44: High Pass CFOA based shadow filter

The corresponding transfer function is:

$$V_O = \frac{s^2 V_1}{s^2 + s\frac{1}{C_2 R_2}(1+G_2) + \frac{1+G_1\left(\frac{R_3}{R_4}\right)}{R_1 R_3 C_1 C_2}} \quad (38)$$

Where $G_1 = R_{b1}/R_{a1}$ and $G_2 = R_{b2}/R_{a2}$.

To verify case#1; the circuit in Fig.44 is implemented experimentally where G_1 is used to tune the center frequency while G_2 is set to zero. The experimental results are summarized in Table20. Fig.45 shows the magnitude and the phase frequency response.

Table 20: The Experimental results for the shadow high Pass filter of Fig.44 (Case#1)

G1	1	2	3	4	5
G2	0	0	0	0	0
R_3/R_4	3.8	3.8	3.8	3.8	3.8
fo	50.1 KHz	69 KHz	83 KHz	92 KHz	103 KHz

In Fig.45, the magnitude response shows peaks as the feedback amplifier's gain increases because as the center frequency of the high pass increases, the quality factor will increases by the same amount.

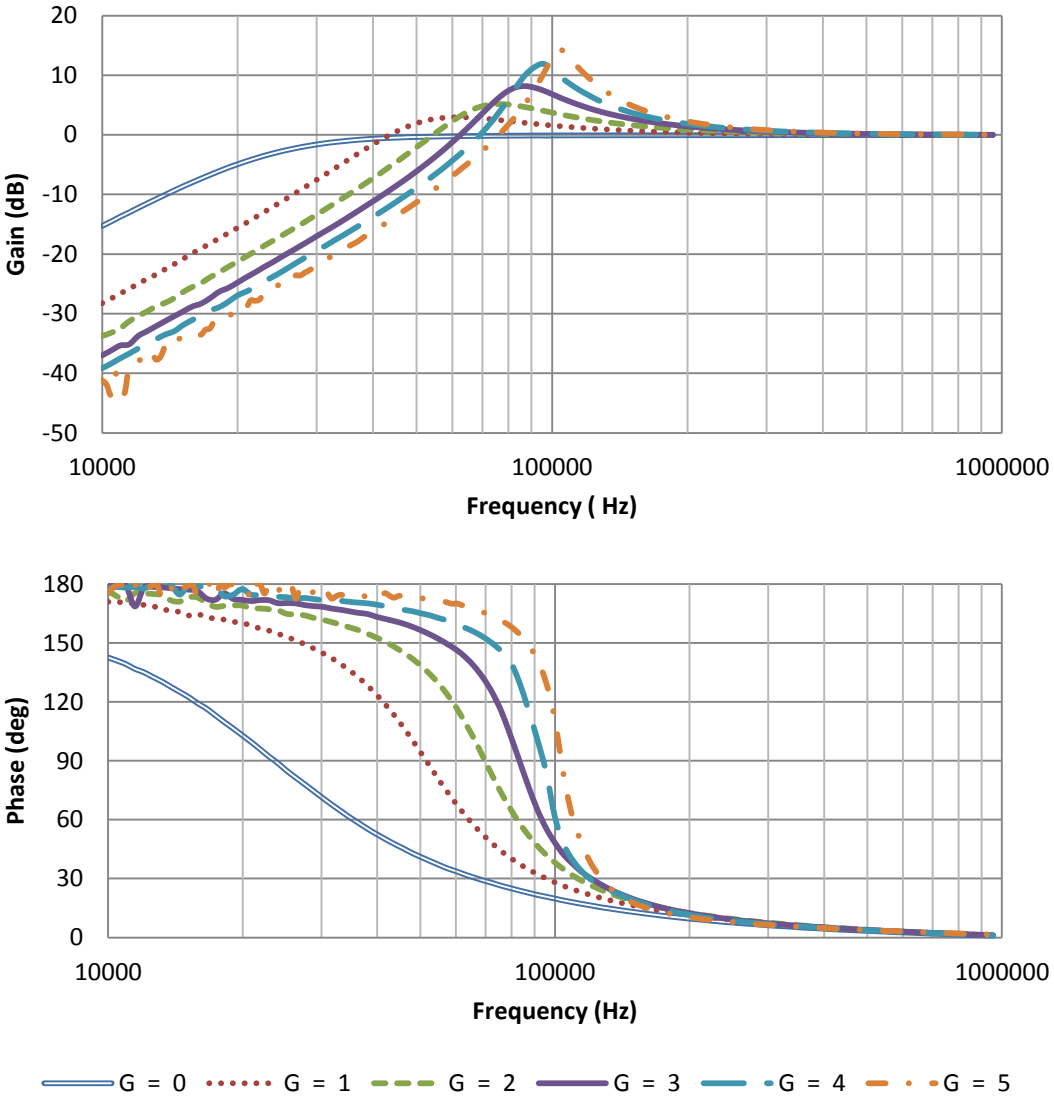

Fig. 45: The gain and the phase frequency response of shadow high Pass filter (Case#1)

B. Case#2:

In case#2; G_1 is used to tune the center frequency of the high pass filter while G_2 is used maintain the quality factor to be $1/\sqrt{2}$ to achieve a high pass filter with flat response.

The quality factor of the original filter (Fig.42) is set to 0.721. In order to keep the quality factor constant during tuning the center frequency, G_1 and G_2 must satisfy:

$$\frac{\sqrt{1 + G_1\left(\frac{R_3}{R_4}\right)}}{(1 + G_2)} = 1 \qquad (39)$$

G_1 is intended to be used to tune the center frequency, so G_2 must satisfy Eq.40 where $R_3/R_4 = 3.84$

$$G_2 = \sqrt{1 + 3.84G_1} - 1 \qquad (40)$$

The experimental results are summarized in Table21. Fig.46 shows the magnitude and the phase frequency response.

Table 21: The Experimental results for the shadow high Pass filter of Fig.44 (Case#2)

	To Maintain $Q = 0.72$				
G_1	1	2	3	4	5
G_2	1.2	1.94	2.5	3	3.5
fo	50.1 KHz	64 KHz	76.4 KHz	87 KHz	95 KHz

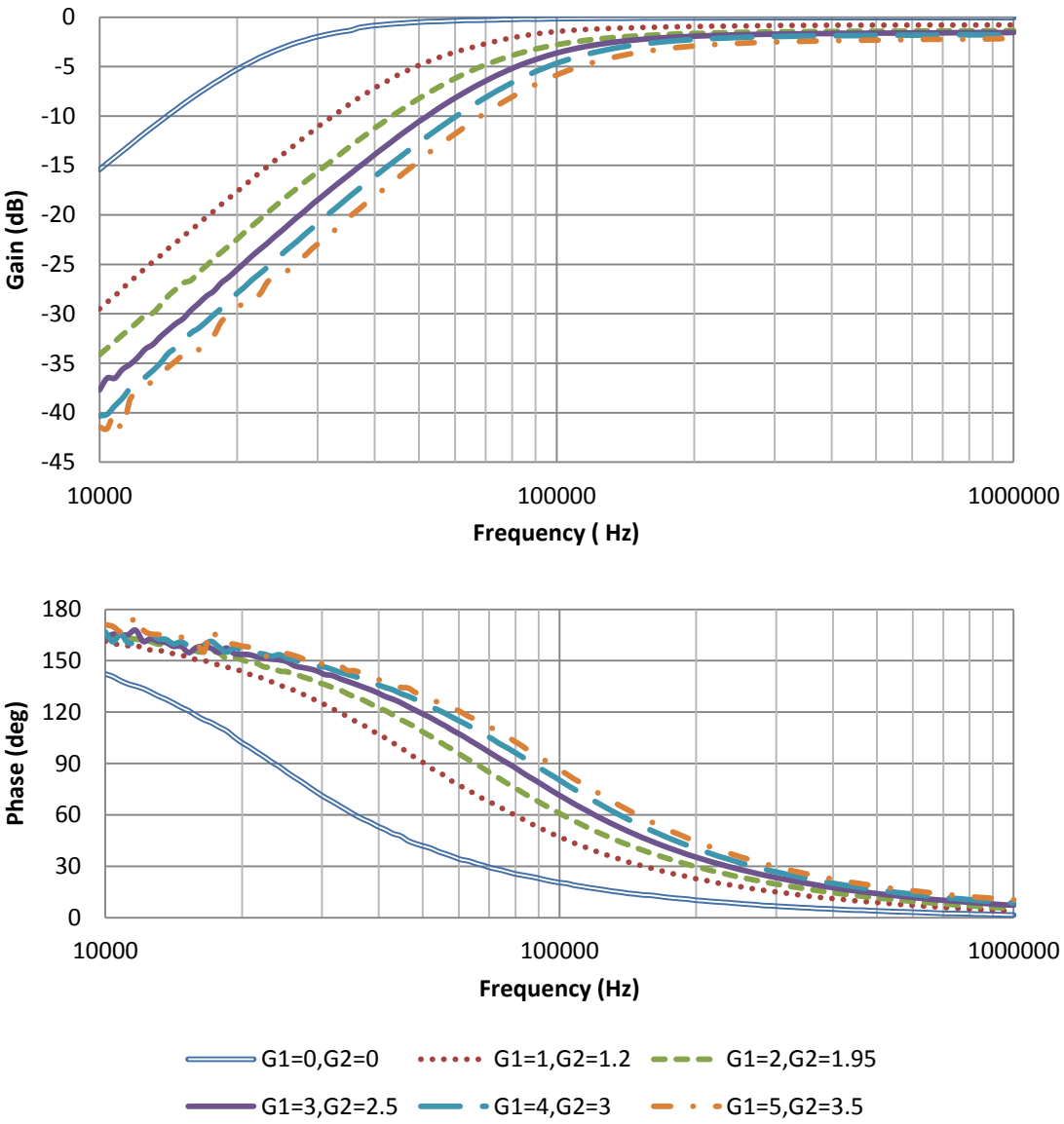

Fig. 46: The gain and the phase frequency response of shadow high Pass filter (Case#2)

3.7 Tuning the Quality Factor and the Center Frequency of the Low Pass Filter:

If the block diagram shown in Fig.40 has the transfer function given by:

$$V_O = \frac{AV_1 + BsV_2 + CV_3}{as^2 + bs + 1} \tag{41}$$

- Low-Pass filter will be realized if $V_1 = V_{IN}$ and $V_2 = V_3 = 0$.
- Band-pass filter will be realized if $V_2 = V_{IN}$ and $V_1 = V_3 = 0$.
- Low-pass filter will be realized if $V_3 = V_{IN}$ and $V_2 = V_1 = 0$.

Fig.47 shows a block diagram for a low pass filter where the quality factor *Q* and the center frequency *fo* is independently controlled by the two external amplifiers G_1 and G_2. The G_3 amplifier is used to maintain the gain of the shadow low pass filter constant because as the center frequency is tuned by $\sqrt{1 - G_1 C}$, the gain of the low pass filter will be reduced by a factor of $1 - G_1 C$ as it is illustrated in Table22.

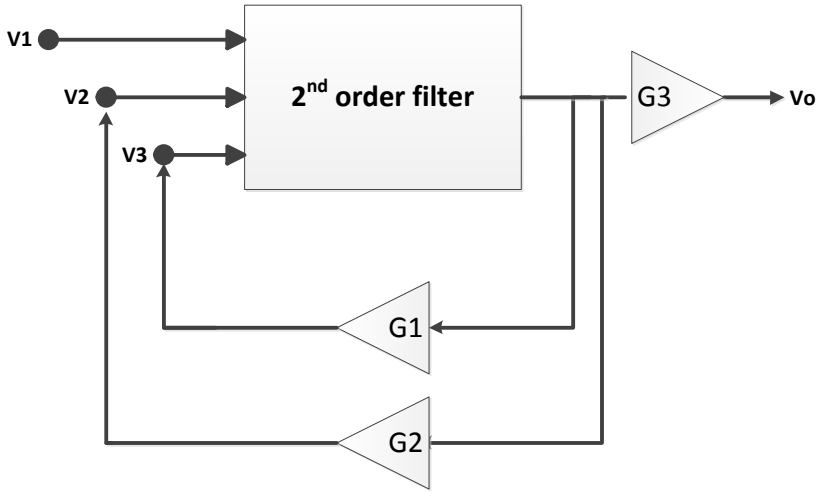

Fig. 47: Shadow Low Pass Filter

$$V_O = \frac{\frac{A}{1 - G_1 C} V_1 G_3}{\frac{as^2}{1 - G_1 C} + \frac{b - G_2 B}{(1 - G_1 C)} s + 1} \quad (42)$$

If the $\boldsymbol{G_3 = 1 - G_1 C}$, The DC gain will remain constant = *A*

Table 22: The shadow low pass parameters

Center Frequency	***Quality Factor***	***High pass Gain***
$\boldsymbol{f_O = \frac{1}{2\pi}\sqrt{\frac{1}{a}\sqrt{1 - G_1 C}}}$	$\boldsymbol{Q = \frac{\sqrt{\frac{1}{a}\sqrt{1 - G_1 C}}}{\frac{b - G_2 B}{a}}}$	$\boldsymbol{G_{LPF} = A}$

G_1 is used to tune the center frequency and in the same time the quality factor will change, so G_2 is used to have control over the quality factor while tuning the center frequency.

3.7.1 Practical verification for tuning fo of the shadow Low Pass Filter:

The practical verification for the shadow low pass filter in Fig.47 is divided into two cases:

A. **Case#1**: G_1 is used to tune the center frequency of the low pass filter while G_2 is set to zero.

B. **Case#2**: G_1 is used to tune the center frequency of the low pass filter while G_2 is used maintain the quality factor to be $1/\sqrt{2}$ to achieve a high pass filter with flat response.

A. **Case#1:**

Consider the circuit in Fig.48, a modified version of [9], which has three inputs and single output with the transfer function in Eq.43

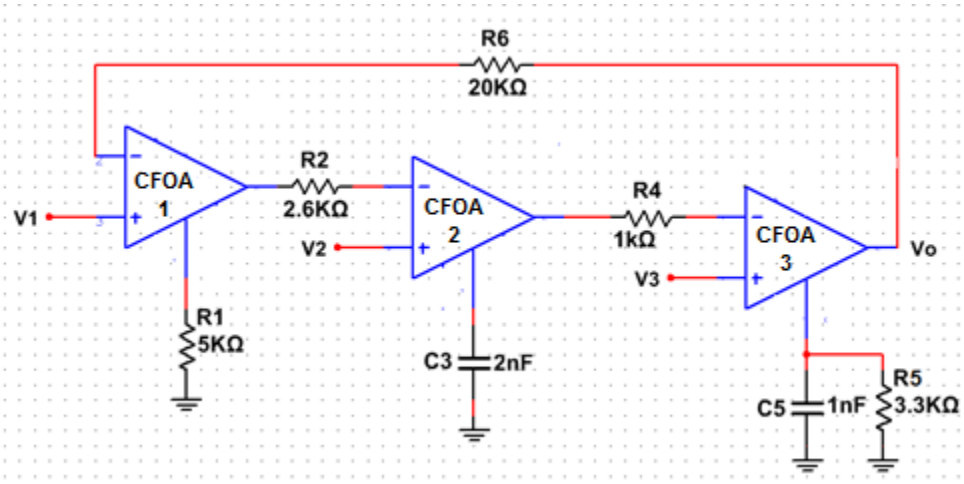

Fig. 48: MISO CFOA Filter [9]

$$V_O = \frac{\frac{R_1}{R_2R_4R_6C_3C_5}V_1 - \frac{1}{R_2R_4C_5C_2}V_2 + s\frac{1}{C_5R_4}V_3}{s^2 + s\frac{1}{C_5R_5} + \frac{R1}{R_2R_4R_6C_3C_5}} \qquad (43)$$

The filter in Fig.48 is implemented in the NI ELVIS II+ breadboard. The inputs V_2 and V_3 set to the ground in order to realize low-pass filter. Table.23 illustrates the theoretical and experimental results.

Table 23: Experimental and Theoretical results Summary

	Theoretical result	Experimental result
fo	34.8 KHz	31.6 KHz
Quality factor	0.723	0.7
G_{LPF}	1	1

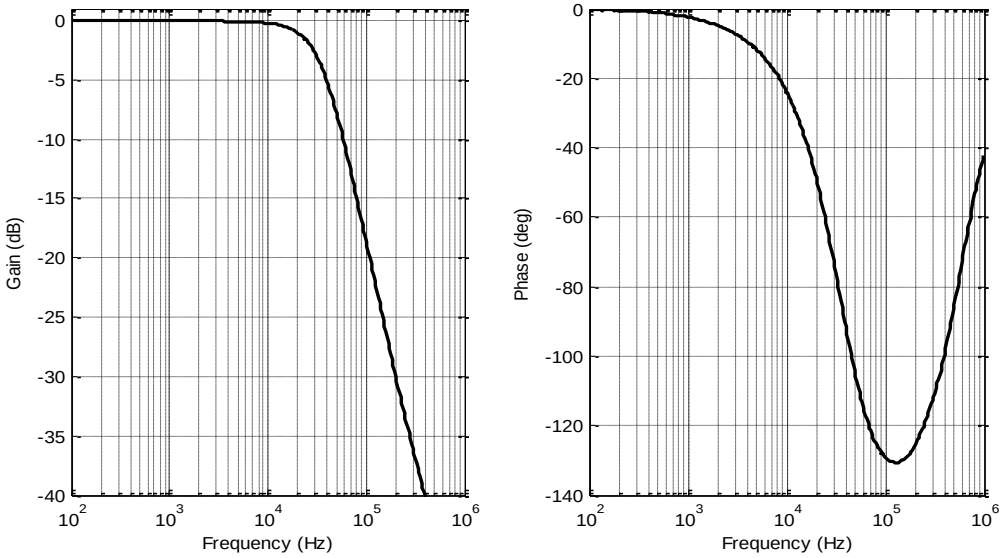

Fig. 49: Gain and Phase frequency response of Fig.48

Now, the two feedback amplifiers are applied from the output to V_2 and V_3 to satisfy the block diagram of Fig.47 as it is illustrated in Fig.50

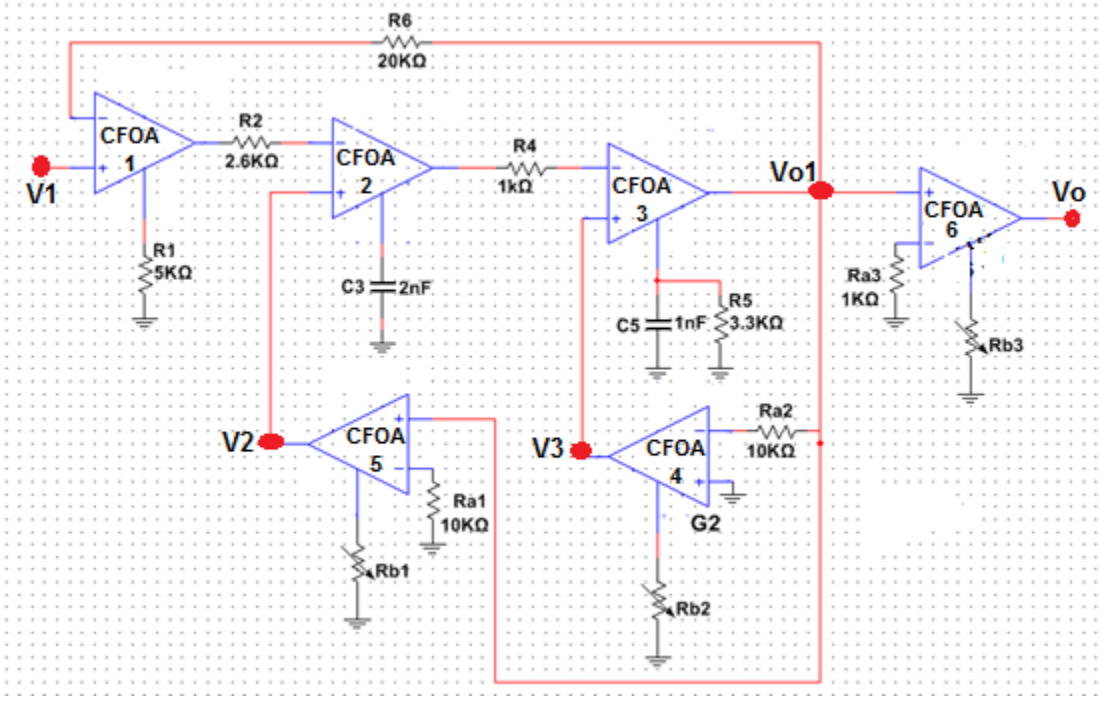

Fig. 50: Low Pass CFOA based shadow filter

The corresponding transfer function is:

$$V_O = \frac{\frac{R_1}{R_2 R_4 R_6 C_3 C_5} V_1 G_3}{s^2 + s\left(\frac{1}{C_5 R_5} + G_2 \frac{1}{C_5 R_4}\right) + \frac{R_1}{R_2 R_4 R_6 C_3 C_5}\left(1 - G_1 \frac{R_6}{R_1}\right)} \quad (44)$$

Where $G_1 = -R_{b1}/R_{a1}$, $G_2 = R_{b2}/R_{a2}$ and $G_3 = -R_{b3}/R_{a3}$.

In order to avoid the gain reduction due to the center frequency tuning, G_3 must be:

$$G_3 = 1 - G_1 \frac{R_6}{R_1} \quad (45)$$

To verify case#1; the circuit in Fig.50 is implemented experimentally where G_1 is used to tune the center frequency while G_2 is set to zero while the gain of the compensation amplifier (G_3) is modified accordingly to maintain equal DC gains for different response . The experimental results are summarized in Table24. Fig.51 shows the magnitude and the phase frequency response.

In Fig.51, the magnitude response shows peaks as the feedback amplifier's gain increases because as the center frequency of the low pass increases, the quality factor will increases by the same amount.

Table 24: Experimental results summary of shadow LPF of Fig.50 (Case#1)

G_1	0	-1	-2	-3	-4	-5
G_2	0	0	0	0	0	0
G_3	0	4.9	7.8	12.7	16.6	20.5
R_6/R_1	3.9	3.9	3.9	3.9	3.9	3.9
fo	31KHz	67 KHz	92 KHz	113.5 KHz	130 KHz	150 KHz

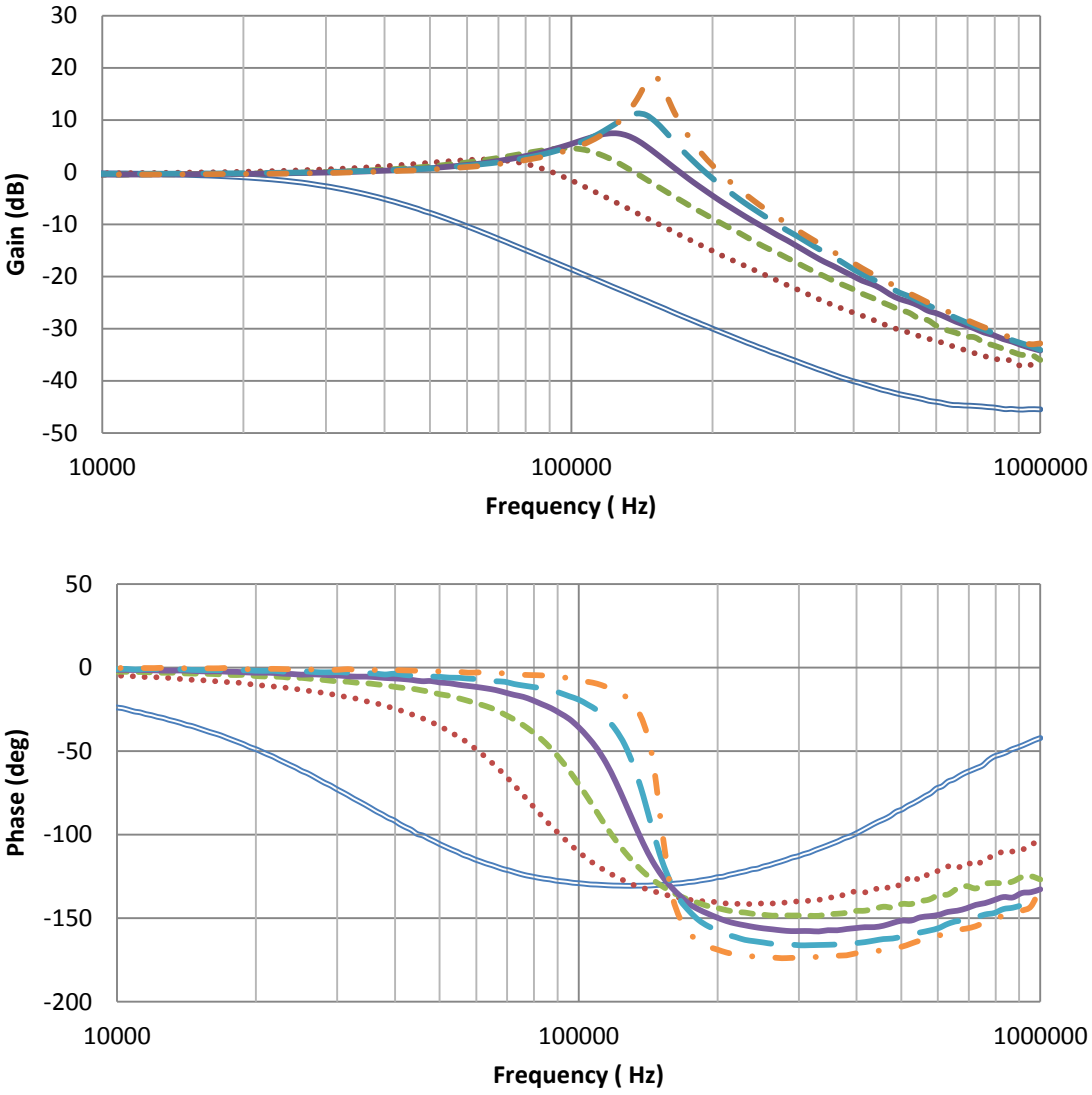

Fig. 51 Gain and Phase frequency response of LPF of Fig.50 (Case#1)

B. **Case#2:**

In case#2; G_1 is used to tune the center frequency of the low pass filter while G_2 is used maintain the quality factor to be $1/\sqrt{2}$ to achieve a low pass filter with flat response.

The quality factor of the original filter (Fig.48) is set to 0.723:

$$Q = \frac{\sqrt{\frac{R_1}{R_2 R_4 R_6 C_3 C_5}}}{\frac{1}{C_5 R_5}} = 0.723 \tag{46}$$

In order to maintain the flat response during tuning the center frequency, the G_1 and G_2 must satisfy Eq.(47):

$$Q = \frac{\sqrt{\frac{R_1}{R_2 R_4 R_6 C_3 C_5}}\sqrt{1 + \frac{R_6}{R_1} G_1}}{\frac{1}{C_5 R_5} + G_2 \frac{1}{C_5 R_4}} = 0.723 \tag{47}$$

Eq.48 can be derived from Eq.47 by taking Q of Eq.46 as common factor from Eq.47 and taking in the consideration R_6/R_1=3.9 and R_5/R_4=3.3.

$$\frac{\sqrt{1 + 3.9 G_1}}{1 + 3.3 G_2} = 1 \tag{48}$$

Eq.48 must be satisfied to maintain the quality factor constant during tuning G_1.

The circuit in Fig.50 is tested using NI ELVIS II+ breadboard for several G_1 and G_2 as explained in Table.25. Fig.52 shows the gain and the phase frequency response.

Table 25: Experimental results summary of shadow LPF of Fig.50 (Case#2)

		To Maintain $Q = 0.72$				
G_1	0	-1	-2	-3	-4	-5
G_2	0	0.367	0.59	0.77	0.93	1.069
G_3	0	4.9	8.8	12.7	16.6	20.5
fo	31KHz	67 KHz	92 KHz	113.5 KHz	130 KHz	150 KHz

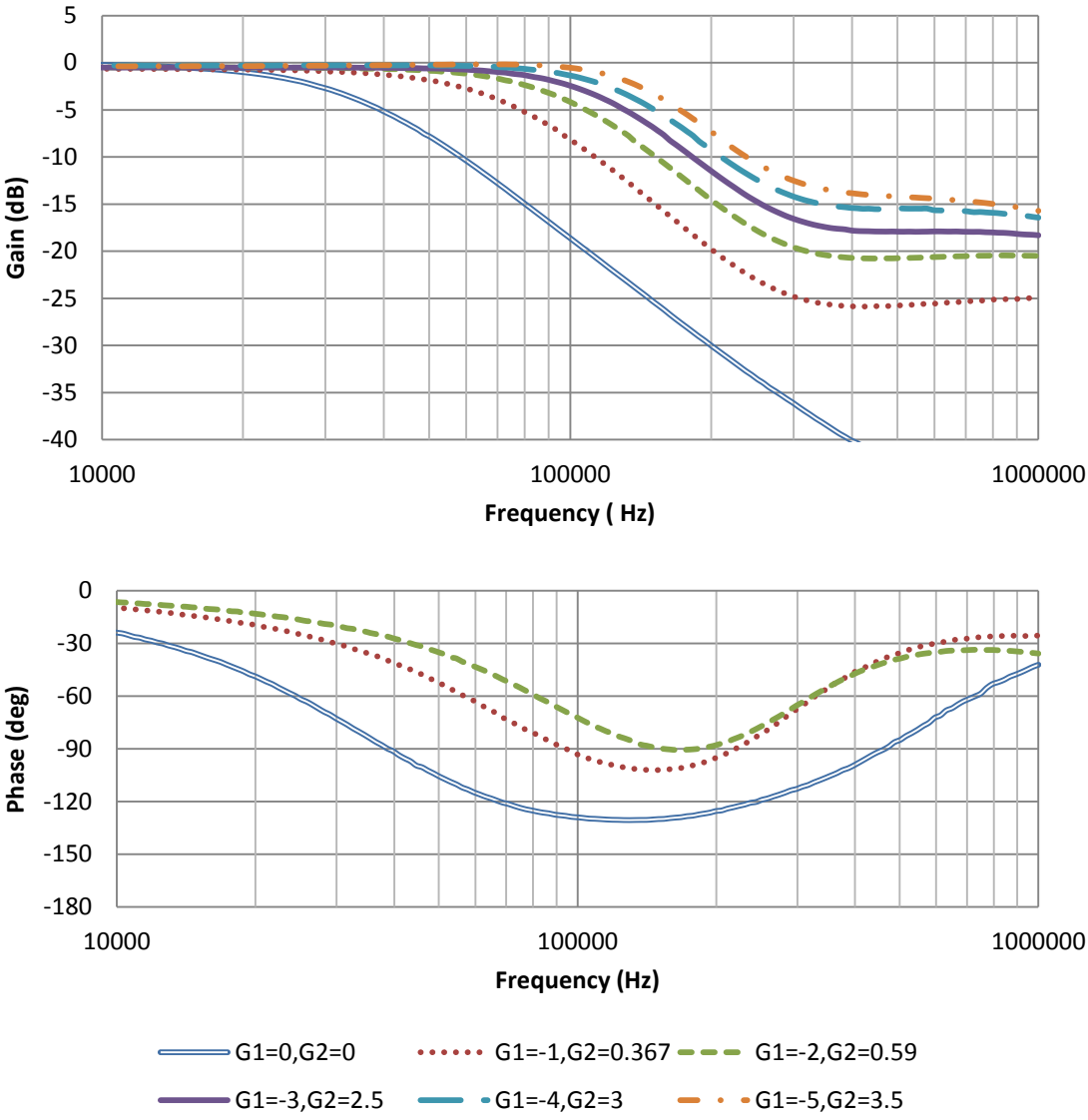

Fig. 52: Gain and Phase frequency response of LPF of Fig.50 (Case#2)

CHAPTER 4

CONCLUSION

The shadow filter theory has been studied and investigated. An extension to the shadow filters theory has been proposed based on the dual input single output filter. Thus, there is no need for an externally connected summing circuit as proposed shadow filter design compared to Fabre's design. In addition to that; a new multi-feedback amplifiers bandpass shadow filter is proposed and tested to give a wider tuning range for the center frequency. Moreover, the idea of the shadow filter has been generalized to include different filter configurations to obtain tunable center frequency with controllable quality factor (Q) as it is explained in the low pass and high pass filters and also tunable quality factor (Q) with constant center frequency as in the notch filter. A new proposed design based on the ideal of the shadow filter is introduced to tune the cut off frequency of the band stop filter.

References

[1] Y. Lakys and A. Fabre, “Shadow filters - new family of second-order filters,” *Electron. Lett.*, vol. 46, no. 4, pp. 276–277, Feb. 2010.

[2] Y. Lakys and A. Fabre, “Shadow filters generalisation to nth-class,” *Electron. Lett.*, vol. 46, no. 14, pp. 985–986, Jul. 2010.

[3] Y. Lakys and A. Fabre, “A fully active frequency agile filter for multistandard transceivers,” in *2011 International Conference on Applied Electronics (AE)*, 2011, pp. 1–7.

[4] V. Biolkova and D. Biolek, “Shadow filters for orthogonal modification of characteristic frequency and bandwidth,” *Electron. Lett.*, vol. 46, no. 12, p. 830, 2010.

[5] N. Pandey, R. Pandey, R. Choudhary, A. Sayal, and M. Tripathi, “Realization of CDTA based frequency agile filter,” in *2013 IEEE International Conference on Signal Processing, Computing and Control (ISPCC)*, 2013, pp. 1–6.

[6] Y. Lakys and A. Fabre, “Multistandard transceivers: state of the art and a new versatile implementation for fully active frequency agile filters,” *Analog Integr. Circuits Signal Process.*, vol. 74, no. 1, pp. 63–78, Jan. 2013.

[7] Y. Lakys and A. Fabre, “Encrypted communications: towards very low consumption frequency-hopping active filters,” *Analog Integr. Circuits Signal Process.*, vol. 81, no. 1, pp. 5–16, Oct. 2014.

[8] M. T. Abuelma'atti, and S.M. Al-Shahrani “New universal filter using two current-feedback amplifiers,” *Int. J. Electron.*, vol. 80, no. 6, pp. 753–756, Jun. 1996.

[9] S. Topaloglu, M. Sagbas, and F. Anday, “Three-input single-output second-order filters using current-feedback amplifiers,” *AEU - Int. J. Electron. Commun.*, vol. 66, no. 8, pp. 683–686, Aug. 2012.

[10] N. Pandey, A. Sayal, R. Choudhary, and R. Pandey, “Design of CDTA and VDTA Based Frequency Agile Filters,” Adv. Electron., vol. 2014, p. e176243, Dec. 2014.

[11] A. M. Soliman, “Applications of the current feedback operational amplifiers,” *Analog Integr. Circuits Signal Process.*, vol. 11, no. 3, pp. 265–302, Nov. 1996.

[12] Hank Zumbahlen. (2008). *Linear Circuit Design Handbook* (1st edition). [On-line]. Available: http://www.analog.com/library/analogDialogue/archives/43-09/linear_circuit_design_handbook.html [3 May 2015].

Vitae

Name	:Naif Radhyan Al-Mutairi
Nationality	:Saudi
Date of Birth	:4/2/1987
Email	:Nayef66@gmail.com
Address	:Al-Dhahran, Saudi Arabia
Academic Background	:M.Sc. and B.Sc. in Electrical Engineering from KFUPM.